

In: *Thalamus*,  
Edited by Steriade, M., Jones, E.G, and McCormick, D.A.  
Elsevier, 1997

**SYNCHRONIZED OSCILLATIONS IN THALAMIC NETWORKS:  
INSIGHTS FROM MODELING STUDIES**

Alain Destexhe<sup>1</sup> and Terrence J. Sejnowski<sup>2,3</sup>

1. Department of Physiology,  
Laval University School of Medicine,  
Québec, G1K 7P4  
Canada

2. Computational Neurobiology Laboratory,  
The Howard Hughes Medical Institute,  
The Salk Institute,  
10010 North Torrey Pines Road,  
La Jolla, California 92037  
USA

3. Department of Biology,  
University of California San Diego,  
La Jolla, California 92037  
USA

Please address correspondence to Dr. A. Destexhe

**Keywords:** *Intrinsic currents, Synaptic receptors, Rebound bursts, Absence epilepsy, Thalamocortical, Thalamic reticular, Sleep spindles, Computational models*

June 10, 1996

2

## Contents

1	INTRODUCTION	3
2	LOW-THRESHOLD SPIKES IN TC AND RE CELLS	3
3	RHYTHMIC FIRING OF SINGLE TC CELLS	5
4	RHYTHMIC FIRING IN SINGLE RE CELLS	9
5	SPINDLE OSCILLATIONS FROM THE TC-RE LOOP	13
6	SPINDLE RHYTHMICITY IN THE ISOLATED RE NUCLEUS	19
7	PAROXYSMAL DISCHARGES IN THE THALAMUS	25
8	DENDRITIC CURRENTS IN THALAMIC NEURONS	28
9	SYNTHESIS	30
10	CONCLUSION	34

## Margin Statements

A T-type  $Ca^{2+}$  current underlies burst firing in TC and RE cells (page 4).

$I_T$ - $I_h$  interaction generates intrinsic slow oscillations in TC cells (page 5)

$Ca^{2+}$ -dependent upregulation of  $I_h$  underlies waxing and waning of oscillations in TC cells (page 8)

$I_T$  and  $I_{K[Ca]}$  generates  $\sim 10$  Hz intrinsic oscillations in RE cells (page 9)

TC-RE interaction generates 8-10 Hz spindle rhythmicity (page 13)

Oscillations can propagate in thalamic (TC-RE) networks (page 17)

A different type of  $\sim 10$  Hz rhythmicity in the RE nucleus is voltage dependent (page 22)

GABA<sub>B</sub> receptors are essential to explain thalamically-generated paroxysmal discharges (page 25)

Burst firing in RE cells is dependent on dendritic  $Ca^{2+}$  currents (page 28)

## 1 INTRODUCTION

The early work of Morison and Bassett (1945) strongly suggested that the thalamus generates coherent rhythmicity in the spindle frequency range (7-14 *Hz*). Since then the cellular correlates of this rhythmicity have been investigated in detail by *in vivo* and *in vitro* techniques (reviewed in Steriade et al., 1993a, and Steriade et al. in this volume). The interaction between thalamocortical (TC) and thalamic reticular (RE) cells is involved in the genesis of this rhythmic activity, but the exact mechanisms are still uncertain and contradictory data remain to be resolved.

Andersen and Rutjord (1964) proposed a model of thalamic rhythmicity over thirty years ago that depended on rebound bursts in thalamic neurons following inhibition. Although the anatomical details of their model need to be revised, and much more is now known about the intrinsic currents of thalamic neurons as well as their synaptic receptors, the primary mechanism for thalamic rhythmicity in their model is now believed to be substantially correct, based on a wide range of experimental and theoretical studies. Computational models have been used to study the dynamical behavior of single thalamic cells, which are sufficiently complex that the consequences of their intrinsic ionic mechanisms are often difficult to predict. Based on precise voltage-clamp data for these ionic currents, well-defined computational models have been used to explore the spatial and temporal organization of coherent rhythmicity in networks of neurons in thalamic nuclei.

In this chapter, we review recent computational models for thalamic oscillations that were developed independently by several investigators. These thalamic models are more mature than those developed for other parts of the mammalian central nervous system, and are as mature as the best models of invertebrate central pattern generators (Selverston, 1985). These advances should lead to deeper insights into the physiological mechanisms of thalamic rhythmicity and form the basis for studying more complex thalamocortical rhythms.

## 2 LOW-THRESHOLD SPIKES IN TC AND RE CELLS

The propensity of TC and RE cells to fire bursts of action potentials is greatly enhanced during the onset of sleep (Steriade and Llinás, 1988). In both TC and RE cells, a voltage-dependent  $Ca^{2+}$  current underlies these bursts of action potentials. Voltage-clamp studies in TC (Coulter et al., 1989) and RE cells (Huguenard and Prince, 1992) have characterized the properties of this T-type  $Ca^{2+}$  current ( $I_T$ ), which is unusual in that the voltage ranges of activation and inactivation are relatively hyperpolarized, in the range of -80 to -50 *mV*. As a consequence,  $I_T$  can be activated below the threshold for action potential generation in both TC and RE neurons, giving rise to low-threshold spikes (LTS).

The presence of  $I_T$  endows TC and RE cells with highly complex response properties. In this section, we summarize Hodgkin-Huxley type of models of  $I_T$  in TC cells (Wang et al. 1991) and RE cells (Destexhe et al. 1993b) based on the kinetics of  $I_T$  (Coulter et al., 1989; Huguenard and Prince, 1992). The generation of the LTS in TC and RE cells, including  $I_T$  and the fast  $Na^+/K^+$  currents responsible for fast action potentials, is shown in Figure 1.

In TC cells, the resting membrane potential is assumed to be near -60 *mV*, in agreement with studies *in vivo* (Deschênes et al., 1984) and *in vitro* (Jahnsen and Llinás, 1984a; McCormick and Pape, 1990a; Leresche et al., 1991). In some cases, however, the resting membrane potential of these cells can be more negative (Soltesz et al., 1991; Huguenard and Prince, 1992). Due to the low activation/inactivation voltage range of  $I_T$ , TC cells easily produce a LTS following injection of a hyperpolarizing current pulses. This rebound-burst property underlies the electrophysiological

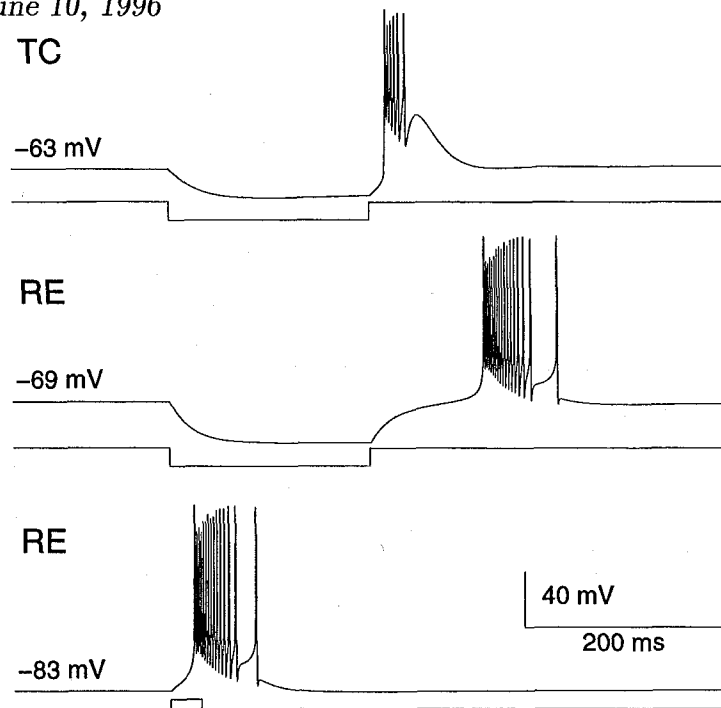


Figure 1:

Low-threshold spikes in thalamocortical and thalamic reticular cells. In these simulations, single-compartment models of TC and RE cells contained a leakage current, the low-threshold  $Ca^{2+}$  current  $I_T$  and the fast  $Na^+/K^+$  currents responsible for action potentials. The TC cell also contained  $I_h$ . Top: rebound burst in a TC cell following hyperpolarizing current injection ( $-0.2$  nA); Middle: rebound burst in a RE cell following hyperpolarizing current injection ( $-0.2$  nA); Bottom: burst in the same RE cell following depolarizing current injection ( $0.1$  nA) starting from a lower resting level which deinactivated  $I_T$ . The parameters of the currents were taken from Destexhe et al., 1993b and Destexhe et al., 1996a, 1996b.

properties of these cells (see elsewhere in this volume). At sufficiently hyperpolarized values,  $I_T$  deinactivates; the return of the membrane potential to around  $-60$  mV is then accompanied by activation of  $I_T$ , which can evoke a burst of action potentials. Simulations of typical rebound bursts are shown in Figure 1.

In RE cells, the activation and inactivation characteristics of  $I_T$  are similar to those in TC cells, but the kinetics were slower and the activation range was more depolarized than that of TC cells (Huguenard and Prince, 1992). Using a Hodgkin-Huxley-type model of  $I_T$  in RE cells, we also simulated the rebound-bursting properties of these cells (Fig. 1). The level of the resting membrane potential of RE cells might be important in understanding the cellular mechanisms of rhythmicity (see later discussion). In Fig. 1, a burst of action potentials could be obtained by depolarizing currents if the RE cell was maintained at a hyperpolarized level.

Many models of LTS generation in TC cells have been proposed (Rose and Hindmarsh, 1985, 1989; Huguenard and McCormick, 1992; Lytton and Sejnowski, 1992; McCormick and Huguenard, 1992; Toth and Crunelli, 1992; Destexhe and Babloyantz, 1993; Destexhe et al., 1993a; Wang and Rinzl, 1993; Wang, 1994; Wallenstein, 1995; Destexhe et al., 1996a). Similar model for RE cells have also been studied (Destexhe and Babloyantz, 1992; Destexhe et al., 1993b; Wang and Rinzl, 1993; Destexhe et al., 1994a; Golomb et al., 1994; Wallenstein, 1994a; Destexhe et al., 1996a, 1996b).

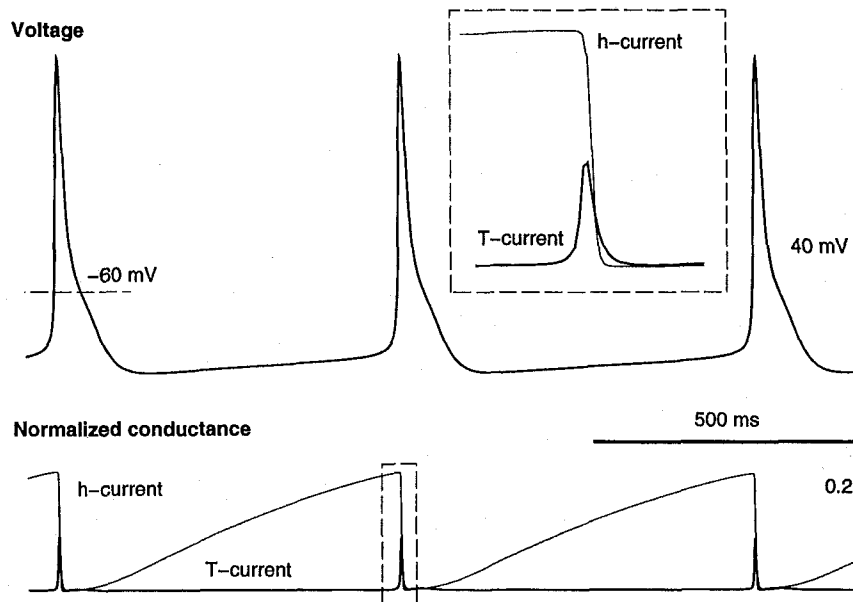


Figure 2:

Slow oscillations in thalamocortical cells from the interaction of two voltage-dependent currents. The model TC cell consisted of a single compartment containing a the minimal set of currents for generating oscillatory behavior (a leakage current, the low-threshold  $Ca^{2+}$  current  $I_T$  and the hyperpolarization-activated current  $I_h$ ; the fast  $Na^+/K^+$  currents responsible for action potentials were not included). Rhythmic oscillations occurred through the interaction between  $I_T$  and  $I_h$ . The bottom curves represent the normalized conductance ( $g/g_{max}$ ) of both currents. The dashed box shows the currents with 8-fold higher time resolution. Note that the T-current activation preceded the h-current deactivation. The parameters of the currents were taken from Destexhe et al., 1993b.

All of these models have corroborated the assumption that the voltage-dependent properties of  $I_T$ , as determined by voltage-clamp experiments, are sufficient to account for the rebound burst response observed in these cells.

### 3 RHYTHMIC FIRING OF SINGLE TC CELLS

In addition to having a prominent rebound-burst property, TC cells also display sustained oscillations. Experiments performed in cats *in vivo* showed that TC cells generate clock-like rhythmicities in the delta range (0.5-4 Hz) after removal of the cortex (Curró Dossi et al., 1992). Oscillations in the same frequency range were also observed in TC cells *in vitro* (Leresche et al., 1990; McCormick and Pape, 1990a; Leresche et al., 1991). These slow frequency oscillations consisted of rebound bursts recurring periodically, and have been called "pacemaker oscillations" (Leresche et al., 1990, 1991).

These slow oscillations were resistant to tetrodotoxin, indicating that they arose from mechanisms intrinsic to the cell. Further *in vitro* electrophysiological investigations have demonstrated the existence of a mixed  $Na^+/K^+$  current,  $I_h$ , that is responsible for anomalous rectification in TC cells (Pollard and Crunelli, 1988; McCormick and Pape, 1990a). In voltage-clamp studies,  $I_h$  is activated by hyperpolarization in the subthreshold range of potentials and is involved in the generation of the slow oscillations of TC neurons (McCormick and Pape, 1990a; Soltesz et al., 1991).

In order to better understand the interplay of  $I_T$  and  $I_h$  in generating oscillatory behavior in TC cells, we developed a kinetic model of this current based on voltage-clamp data (Destexhe

and Babloyantz, 1993); the kinetic scheme was similar to that introduced by Hodgkin and Huxley (1952) for the fast sodium current, but with two independent activation mechanisms instead of one and no inactivation. This kinetic model faithfully reproduced voltage-clamp data showing the slow activation and rapid deactivation that is typical of  $I_h$  (McCormick and Pape, 1990a).

The combination of  $I_T$  and  $I_h$  produces robust oscillations (Fig. 2), as suggested by *in vitro* experiments (McCormick and Pape, 1990a; Soltesz et al., 1991) and confirmed by a number of modeling studies (Lytton and Sejnowski, 1992; McCormick and Huguenard, 1992; Toth and Crunelli, 1992; Destexhe and Babloyantz, 1993; Destexhe et al., 1993a; Wang, 1994; Lytton et al., 1996b). In Figure 2, we have represented the membrane potential together with the normalized conductance of the two currents  $I_T$  and  $I_h$ . The increase of membrane potential during an LTS deactivates  $I_h$  relatively rapidly. The resulting hyperpolarization then slowly reactivates  $I_h$ , which progressively increases the membrane potential until a new LTS occurs, and the cycle repeats.

In TC cells from cat studied in low- $Mg^{2+}$  medium *in vitro*, a few cells displayed waxing-and-waning slow-frequency oscillations. These 0.5-3.2 Hz oscillations were composed of periods of 1-28 s of oscillation that waxed and waned, separated by silent phases of 5-25 s duration. The waxing-and-waning was resistant to tetrodotoxin, suggesting mechanisms intrinsic to the TC neuron. By analogy with the waxing-and-waning of *in vivo* spindles, they have also been called "spindle-like oscillation" (Leresche et al., 1990, 1991). However, *in vivo* spindles occur at a much higher intraburst frequency (7-14 Hz) and depend on interactions with neurons of the thalamic reticular nucleus (Steriade and Deschênes, 1984; Steriade et al., 1985, 1987, 1990), so they are quite distinct from the waxing-and-waning slow oscillations seen *in vitro*. *In vivo* recordings of TC cells also show periods of waxing-and-waning slow oscillations (see Fig. 12 in Steriade et al., 1993b).

Slow oscillations and waxing-and-waning oscillations can be observed in the same TC cell by altering the h-current (Soltesz et al., 1991). Increasing the amplitude of  $I_h$  by noradrenaline can transform slow oscillations into waxing-and-waning oscillations; application of  $Ca^{2+}$ , an  $I_h$  blocker, has the opposite effect (Soltesz et al., 1991). No other current seems to be required to produce waxing-and-waning oscillations and interactions between  $I_T$  and  $I_h$  are sufficient to produce them (Soltesz et al., 1991).

As initially proposed by McCormick (1992), it is possible that a  $Ca^{2+}$  regulation of  $I_h$  is involved in the genesis of waxing-and-waning oscillations. The model we studied was based on the  $Ca^{2+}$  modulation of  $I_h$  in sino-atrial node cells (Hagiwara and Irisawa, 1989), suggesting that  $Ca^{2+}$  ions directly bind to  $I_h$  channels. A more recent investigation provided evidence for a  $Ca^{2+}$  modulation of  $I_h$  in neocortical pyramidal cells (Schwindt et al., 1992).  $Ca^{2+}$  ion may not bind directly to  $I_h$  channels (Zaza et al., 1991) and an indirect modulation is more likely. Cyclic AMP may be a good candidate since  $Ca^{2+}$  is actively involved in regulating adenylate cyclase activity (reviewed in MacNeil et al., 1985), and  $I_h$  is sensitive to cyclic AMP (McCormick and Pape, 1990b; Akasu and Tokimasa, 1992; DiFrancesco and Mangoni, 1994). The kinetics of this indirect modulation must be slow, similarly to the  $Ca^{2+}$ -dependent regulation of other types of channels. For example, a kinetic analysis of the slow inactivation of NMDA receptors by intracellular  $Ca^{2+}$  (Legendre et al., 1993) reported relatively fast binding and very slow unbinding rates with a time constant of about 5 s. Direct measurements of  $Ca^{2+}$  binding to  $I_h$  channels have not yet been made in thalamic neurons.

In order to check the plausibility of  $Ca^{2+}$  involvement in waxing-and-waning, we have developed simple kinetic models for the binding of  $Ca^{2+}$  ions to the open form of the  $I_h$  channel, either directly (Destexhe et al., 1993a) or via a calcium-binding protein (Destexhe et al., 1996a). These models reproduced the  $Ca^{2+}$ -dependent shift of the activation curve of  $I_h$  observed in measurements from sino-atrial node cells (Hagiwara and Irisawa, 1989). A slow unbinding rate was used, consistent

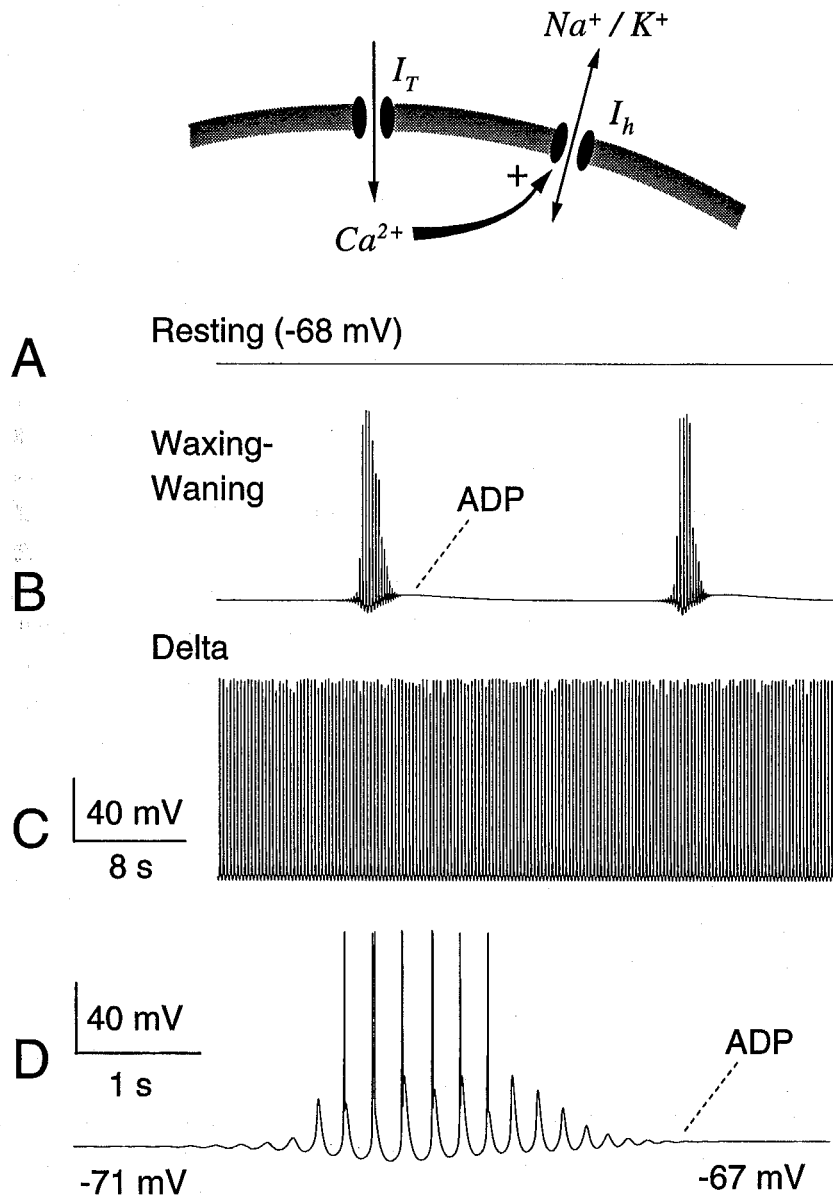


Figure 3:

Modes of rhythmic bursting in single thalamocortical cells that arise from the interplay of the  $I_T$  and  $I_h$  currents. This model consisted of a single compartment with a leakage current,  $Na^+/K^+$  currents responsible for action potentials,  $I_T$ ,  $I_h$  and a  $Ca^{2+}$  regulation of  $I_h$ , as schematized above. The membrane potential in the model is shown for (A) resting behavior around -68 mV, (B) waxing-and-waning oscillations at 3.5-4.5 Hz with silent periods of 4 to 20 s, and (C) sustained oscillations at 0.5-4 Hz. Waxing and waning oscillations are shown at higher magnification in D. A-B-C were obtained by successively decreasing the maximal conductance of  $I_h$ . Modified from Destexhe et al., (1996a).

with other kinetic studies of a similar type of regulation (Legendre et al., 1993). As shown in Fig. 3, the combination of  $I_T$  and  $Ca^{2+}$ -dependent  $I_h$  accounts for the waxing-and-waning of the slow oscillations (Destexhe et al., 1993a, 1996a). The mechanism by which these oscillations arise is the following: the TC cell starts to oscillate due to its intrinsic rhythmic properties. During the oscillatory period,  $Ca^{2+}$  enters at each burst and binds to  $I_h$ , augmenting its conductance more and more as the oscillations proceed. The oscillations cease when the depolarization induced by  $Ca^{2+}$ -bound  $I_h$  prevent sufficient deinactivation of  $I_T$ . During the silent period  $Ca^{2+}$  unbinding from  $I_h$  channels slowly repolarizes the membrane (as observed *in vitro* by Leresche et al., 1991) until the oscillations can start again. For a more detailed analysis of the ionic mechanisms underlying these oscillations, see Destexhe et al., 1993a, 1996a.

A progressive reduction of  $I_h$  conductance transformed sustained oscillations into waxing-and-waning oscillations (Fig. 3), following the same progression observed in TC cells *in vitro* (Soltesz et al., 1991). Dynamical systems analysis using a phase plane diagram showed that the waxing-and-waning oscillations arose when  $I_h$  entrained the system alternately between stationary and oscillating branches (Destexhe et al., 1993a). The coexistence of the different modes could also be explained by the same diagram.

Other models have been proposed to account for the waxing-and-waning oscillations in TC cells, in addition to the hypothesis that  $Ca^{2+}$  regulates  $I_h$  (Crunelli et al., 1993). Wallenstein (1995) has considered self-regulation of  $I_h$  by adenosine released in an activity-dependent manner. However, the adenosine-dependence of  $I_h$  in TC cells (Pape, 1992) produces a progressive depolarization during the interspindle silent period, which is inconsistent with the progressive hyperpolarization observed experimentally (Leresche et al., 1991; Bal and McCormick, 1995). Other mechanisms might be responsible for these oscillations, such as an *indirect* regulation of  $I_h$  by  $Ca^{2+}$ , which might occur through other second messengers, or calcium-binding proteins (Destexhe et al., 1996a). It was recently reported that hyperpolarization by current injection during the silent period can reset the spindling behavior (T. Bal. and D.A. McCormick, personal communication), suggesting a voltage-dependence to the mechanism responsible for the slow recovery.

Another class of model for waxing and waning oscillations is based on the interaction between  $I_T$ ,  $I_h$  and a slow potassium current  $I_{K2}$  (Destexhe and Babloyantz, 1993), or on the interactions between  $I_T$ ,  $I_h$  and a  $Ca^{2+}$ -activated potassium current  $I_{K[Ca]}$  (Destexhe and Babloyantz, 1993; Hindmarsh and Rose, 1994b). Although these models were based on currents identified in TC cells, and despite the presence of a progressive hyperpolarization during the interspindle period, the frequency exhibited was on the order of 10 Hz, which is much higher than the 0.5-4 Hz frequency range observed experimentally (Leresche et al., 1991).

In summary, the whole spectrum of resting and oscillatory states observed in TC cells *in vitro* can be reproduced from model based on the interaction of  $I_T$ ,  $I_h$  and intracellular  $Ca^{2+}$ . The dynamics depends on the amplitude of  $I_h$  conductance: (a) For very weak values of the  $I_h$  conductance, the cell has a stable hyperpolarized resting state, close to -80 mV. (b) For weak to moderate  $I_h$  conductances, the interplay of  $I_T$  and  $I_h$  produces oscillations in the delta frequency range (0.5-4 Hz). (c) For higher  $I_h$  conductances, the slow oscillations wax and wane with inter-spindle periods on the order of tens of seconds. (d) For the highest  $I_h$  conductances, the TC cell maintains a depolarized resting state around -60 mV. This latter state is the closest to the threshold for action potentials.

These four modes of activity of the TC cells were reproduced when  $I_h$  was modeled by double-activation kinetics regulated by intracellular  $Ca^{2+}$ . Such a double activation component was recently observed from voltage-clamp measurements of  $I_h$  in other neurons (Solomon and Nerbonne, 1993; Solomon et al., 1993). However, a more conventional activation scheme for the voltage-dependence

of  $I_h$  together with  $Ca^{2+}$  regulation gave rise to similar patterns of activity (Destexhe et al., 1996a).

Since the whole spectrum of oscillatory states is accessible in the same TC cell through changes in  $I_h$ , this current becomes a pressure point for regulation. This current is a known target for many neuromodulators, including noradrenaline and serotonin (McCormick and Pape, 1990b; Soltesz et al., 1991), histamine (McCormick and Williamson, 1991), adenosine (Pape, 1992), and opioids (Ingram and Williams, 1994). These neuromodulators probably act through cyclic AMP, as suggested by the marked effect of cyclic AMP on the voltage-dependence of  $I_h$  (DiFrancesco and Mangoni, 1994). These data and models are consistent with the hypothesis that the control of arousal by these neuromodulators (McCormick, 1992; Chapters 8 and 9 in Volume 1 of this series) operates on TC cells mainly by modulating  $I_h$  and leak  $K^+$  currents. The models suggest that the modulation of  $I_h$  is in a critical position to control the different types of resting and oscillatory modes of these neurons.

## 4 RHYTHMIC FIRING IN SINGLE RE CELLS

RE neurons, like TC cells, are characterized by rhythmic firing properties, but in contrast to TC cells, they rarely display sustained oscillations. Typically, sequences of rhythmic bursts at 7-12 Hz can be evoked by injection of current pulses (Avanzini et al., 1989; Bal and McCormick, 1993), or by stimulating excitatory afferents (Contreras et al., 1993; Huguenard and Prince, 1994b).

The resistance of these oscillations to tetrodotoxin indicates that they are due to mechanisms intrinsic to the cell. Recordings from RE neurons *in vitro* revealed the presence of  $I_T$  and two  $Ca^{2+}$ -activated currents, a  $K^+$  current,  $I_{K[Ca]}$ , and a non-specific cation current,  $I_{CAN}$ , both with slow kinetics (Bal and McCormick, 1993).  $I_{K[Ca]}$  and  $I_{CAN}$  are likely to be activated in the same range of subthreshold membrane potentials within which  $Ca^{2+}$  enters through  $I_T$  channels. *In vitro* experiments show that the rhythmic behavior of RE cells arises from the interaction between  $I_T$ ,  $I_{K[Ca]}$  and  $I_{CAN}$  (Bal and McCormick, 1993).

We have modeled oscillatory behavior in RE cells and included simple kinetic schemes for  $I_{K[Ca]}$  and  $I_{CAN}$  (Destexhe et al., 1993b), in which  $Ca^{2+}$  ions directly bind to the closed form of the channel leading to its opening. The kinetic rates of activation/deactivation of these currents were fit to voltage-clamp and current-clamp recordings of RE cells (Huguenard and Prince, 1992; Bal and McCormick, 1993).

As suggested by current-clamp experiments in RE cells (Avanzini et al., 1989), the interplay of  $I_T$  and  $I_{K[Ca]}$  produces rhythmic oscillations. The model indeed demonstrates that the combination of these two currents can produce very robust rhythmic bursting (Fig. 4). In this case, the rhythmical activity depends on the  $Ca^{2+}$  entry following a LTS:  $Ca^{2+}$  activates  $I_{K[Ca]}$ , which then hyperpolarizes the membrane and deinactivates  $I_T$ . When the membrane depolarizes due to the deactivation of  $I_{K[Ca]}$ , a new LTS is produced and the cycle repeats. The robustness of this mechanism was confirmed in several modeling studies (Destexhe et al., 1993b; Wang and Rinzel 1993; Destexhe et al., 1994a; Hindmarsh and Rose, 1994a; Wallenstein, 1994a).

Another characteristic of RE cells is that the sequence of bursts is often terminated by a tonic tail of spikes, as observed *in vitro* (Avanzini et al., 1989; Bal and McCormick, 1993) and *in vivo* (Domich et al., 1986; Contreras et al., 1993). Bal and McCormick (1993) have suggested that this behavior can be explained by the slow activation of the nonspecific cation current,  $I_{CAN}$ .

In the model, the activation of  $I_{CAN}$  accelerated the rising phase of the burst and increased the frequency of the rebound burst sequence. The presence of  $I_{CAN}$  also terminated the oscillatory behavior by producing a tonic tail of spikes before the membrane returned to its resting level. The

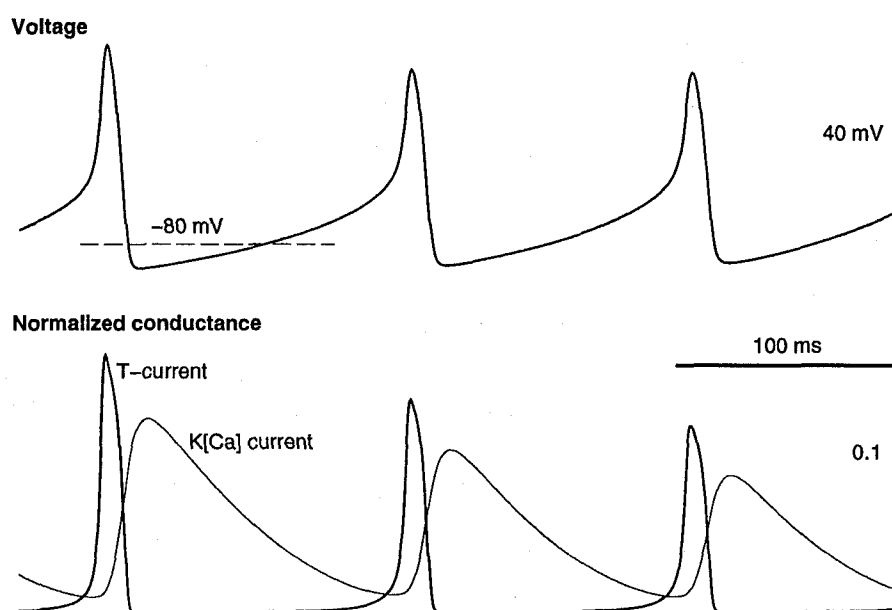


Figure 4:

Model of rhythmic oscillations in single thalamic reticular cells. This simulation was performed with a model based on a single compartment containing a minimal set of currents for generating oscillatory behavior ( $I_T$ ,  $I_{K[Ca]}$ ,  $I_{CAN}$  and submembranal  $Ca^{2+}$ ; fast  $Na^+/K^+$  currents for generating action potentials were not included). The interplay between the two currents  $I_T$  and  $I_{K[Ca]}$  is responsible for this type of oscillatory behavior. The bottom curves represent the normalized conductance ( $g/g_{max}$ ) for these currents. The kinetic parameters of the currents can be found in Destexhe et al., 1993b, 1994a.

relative values of  $\bar{g}_{K[Ca]}$  and  $\bar{g}_{CAN}$  modulated both the frequency and the relative importance of rhythmic bursting relative to tonic tail activity (Fig. 5; Destexhe et al., 1993b; 1994a). These results were confirmed in another modeling study (Wallenstein, 1994a).

The firing pattern of RE cells is under the control of several neuromodulators (reviewed in McCormick, 1992). Electrophysiological experiments have shown that acetylcholine affects the firing pattern of RE cells by activating a leak  $K^+$  current (McCormick and Prince, 1986) whereas noradrenaline (NE) and serotonin (5HT) depolarize thalamic cells by blocking a leak  $K^+$  current (McCormick and Wang, 1991). We consider here the action of NE and 5HT on the firing properties of RE cells through leak  $K^+$  currents, while other possible effects of these neuromodulators were not considered.

Both detailed and simplified models of the G-protein transduction mechanism mediating the action of neuromodulators such as NE and 5HT were included in a recent modeling study (Destexhe et al., 1994d). The simplified kinetic scheme assumed that the opening of the  $K^+$  channel was slow compared to the time course of G-protein activation, and the time course of the second messenger was a pulse of long duration (80 to 100 ms). This simplified model was able to accurately fit averaged  $GABA_B$  currents (Destexhe et al., 1994d), which share a similar G protein-based activation mechanism.

In a similar model of a single RE cell, the leak  $K^+$  current, active at rest, was placed under the control of NE/5HT synapses. We considered three different levels of NE/5HT activity (Fig. 6). First, a hyperpolarized resting level of -65 to -75 mV, similar to *in vitro* conditions where no NE/5HT synapses are activated (Fig. 6). In the second case had a more depolarized resting level of -60 to -70 mV, in which about 20% of the leak  $K^+$  current was blocked. This depolarized resting potential

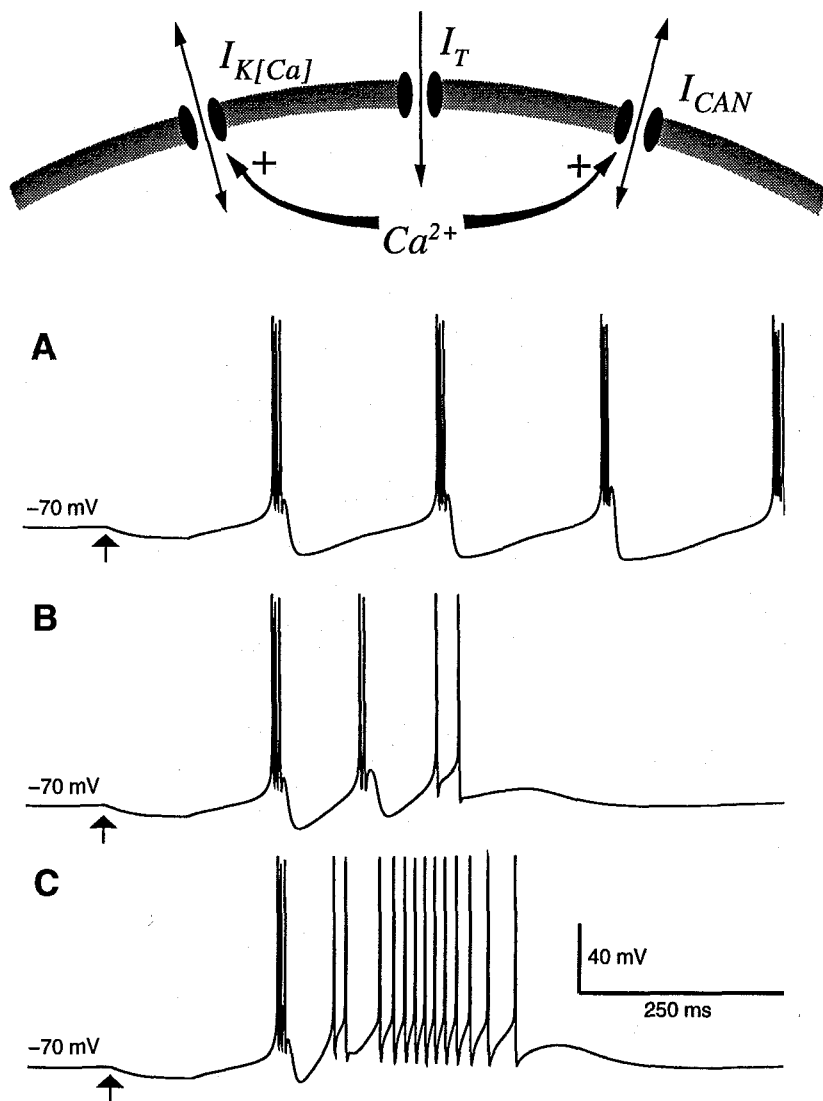


Figure 5:

Rhythmic firing patterns in thalamic reticular neurons modeled by the interplay between three intrinsic currents. These simulations included the currents used in Fig. 4, and the fast  $Na^+/K^+$  currents responsible for action potentials were added. Rhythmic bursting occurred following the interaction between  $I_T$ ,  $I_{K[Ca]}$  and  $I_{CAN}$  (see scheme above). The rebound bursts were evoked by injection of a hyperpolarizing current pulse (arrow). The character of the rhythmic bursts depended on the relative values for the conductances of  $I_{K[Ca]}$  and  $I_{CAN}$ : (A) Rhythmic bursting in the absence of  $I_{CAN}$ ; (B) rhythmic bursting for weak  $I_{CAN}$ ; and (C) rhythmic bursting having a prominent tonic tail of spikes for stronger  $I_{CAN}$ . Modified from Destexhe et al., 1994a.

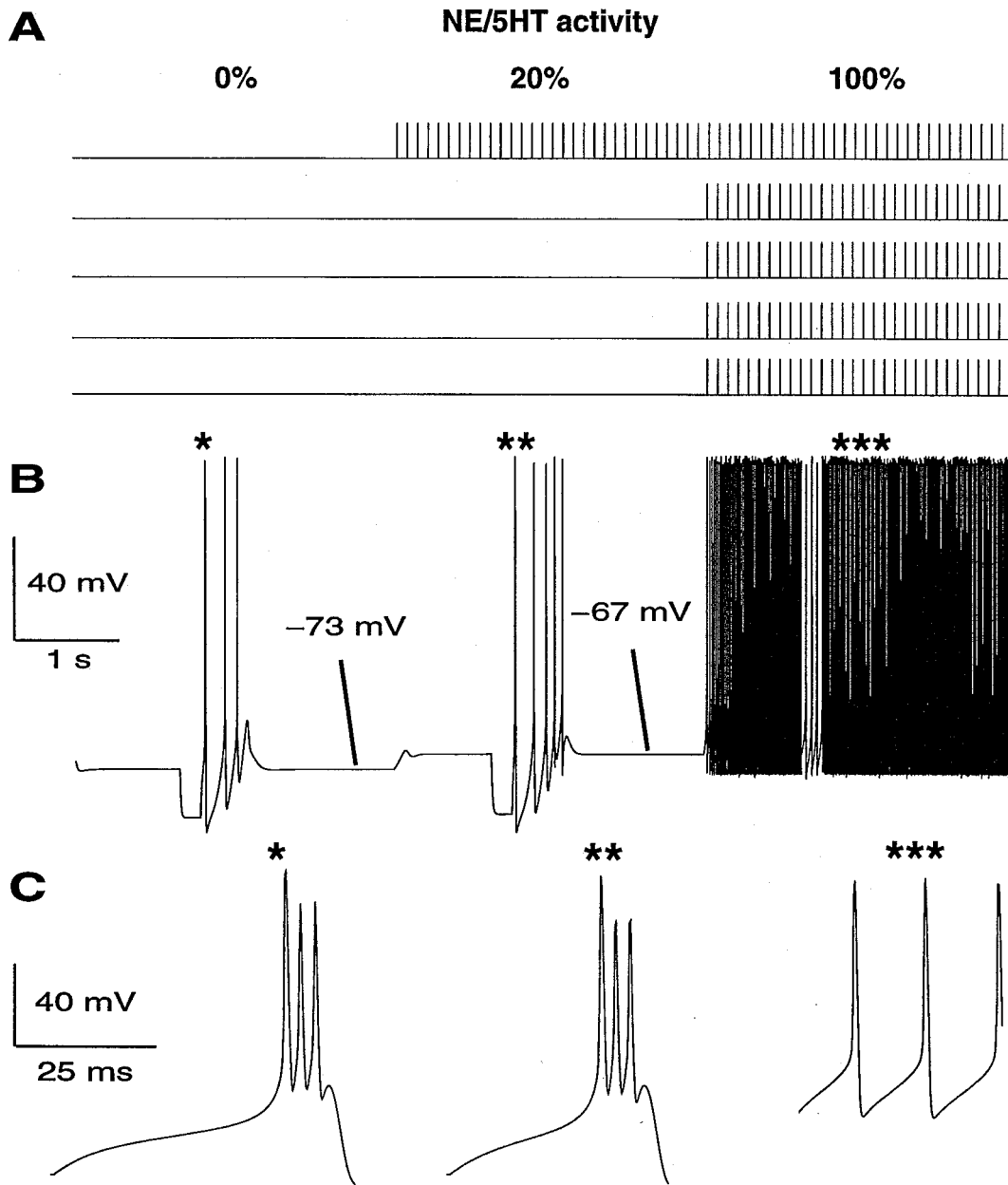


Figure 6:

Noradrenergic/serotonergic regulation of the firing mode of thalamic reticular cells. Simulation of a single RE cell with five noradrenergic synapses. (A) Five top traces show the presynaptic activity of the NE/5HT synapses. (B) Membrane potential of the RE cell. (C) Bursts of action potentials shown at higher temporal resolution. Three successive 3-second periods of different level of NE/5HT activity are shown, during which a hyperpolarizing current pulse was injected; the two first pulses elicited repetitive bursting response whereas the third pulse only slowed the frequency of repetitive spiking. Modified from Destexhe et al., 1994b.

corresponded to weak NE/5HT activity (one out of five synapses was activated). In the third case, when all NE/5HT synapses were activated, a tonic spike activity resulted from the block of virtually all leak  $K^+$  current in the cell (Fig. 6B).

These three states correspond to different modes of intrinsic firing properties of the RE cell: for both hyperpolarized and depolarized resting states, injection of hyperpolarizing current pulses resulted in a sequence of rebound bursts occurring rhythmically at a frequency of 6-10  $Hz$  (Fig. 6). This bursting activity resulted from the interaction between  $I_T$  and  $I_{K[Ca]}$ , as described previously. During tonic spike activity, injection of the same current pulse only slowed down the frequency of action potentials.

In summary, the simple kinetic schemes in the RE model can account for the most salient features of the rhythmic properties of these cells. The different types of firing patterns that have been observed can be understood as arising from different balances between the conductances of  $I_T$ ,  $I_{K[Ca]}$  and  $I_{CAN}$ . These currents organize bursting oscillations in the 9-11  $Hz$  frequency range, which terminate in a tonic tail. In addition, the control of leak  $K^+$  conductances by neuromodulators can switch the cell between tonic and bursting activity.

## 5 SPINDLE OSCILLATIONS FROM THE TC-RE LOOP

In this section, we show how computer models can be used to explore possible mechanisms of interaction between two types of cells having complex firing properties, namely TC and RE cells. In particular, we investigate the genesis of spindle oscillations based on recordings in ferret thalamic slices (von Krosigk et al., 1993; Bal et al., 1995a, 1995b). These *in vitro* spindles consisted of sequences of 5-9  $Hz$  rhythmic bursting separated by silent periods of 3 to 30  $s$ . The occurrence of these spindles depended critically upon the presence of both TC and RE cells and the integrity of synaptic connections between them.

Models of synaptic currents were based on the kinetics of postsynaptic receptors (Destexhe et al., 1994c, 1994d). In patch-clamp experiments with fast perfusion techniques, short pulses of artificially-applied neurotransmitter evoked synaptic currents similar to those observed in intact synapse when pulses of 1  $ms$  duration and 1  $mM$  (Colquhoun et al., 1992) were used. In the model, a brief pulse of neurotransmitter was released from presynaptic neuron whenever a spike occurred; the neurotransmitter then increased transiently the opening of ionic channels of the postsynaptic receptors. Simple kinetic schemes reproduced accurately the time course of several types of postsynaptic receptors, such as the glutamate AMPA/kainate and NMDA types, or the GABAergic GABA<sub>A</sub> receptor (Destexhe et al., 1994d). The models were directly fit to postsynaptic currents obtained in whole-cell recordings from hippocampal neurons.

We first studied a simple circuit that consisted of a pair of interconnected TC and RE cells, as shown in Fig. 7A. The excitatory synapse from the TC cell to the RE cell was mediated by AMPA/kainate glutamate receptors and the inhibitory synapse from the RE to the TC cell was modeled by GABA<sub>A</sub> receptors as identified in ferret thalamic slices (von Krosigk et al., 1993). The PSPs corresponding to these currents are shown in Fig. 7B.

An interacting pair of cells in the model exhibited 8-10  $Hz$  waxing-and-waning oscillations (Fig. 7C-D). The TC and RE cells in the model showed mirror images that are typical of during sleep spindles observed in intracellular recordings of thalamic cells in different preparations (Steriade and Llinás, 1988; von Krosigk et al., 1993). The spindle oscillations began in the TC cell in a manner very similar to the waxing-and-waning slow oscillations of isolated TC cells (compare to Fig. 3B). As the oscillation began, the first burst of spikes in the TC cell elicited a series of excitatory PSPs

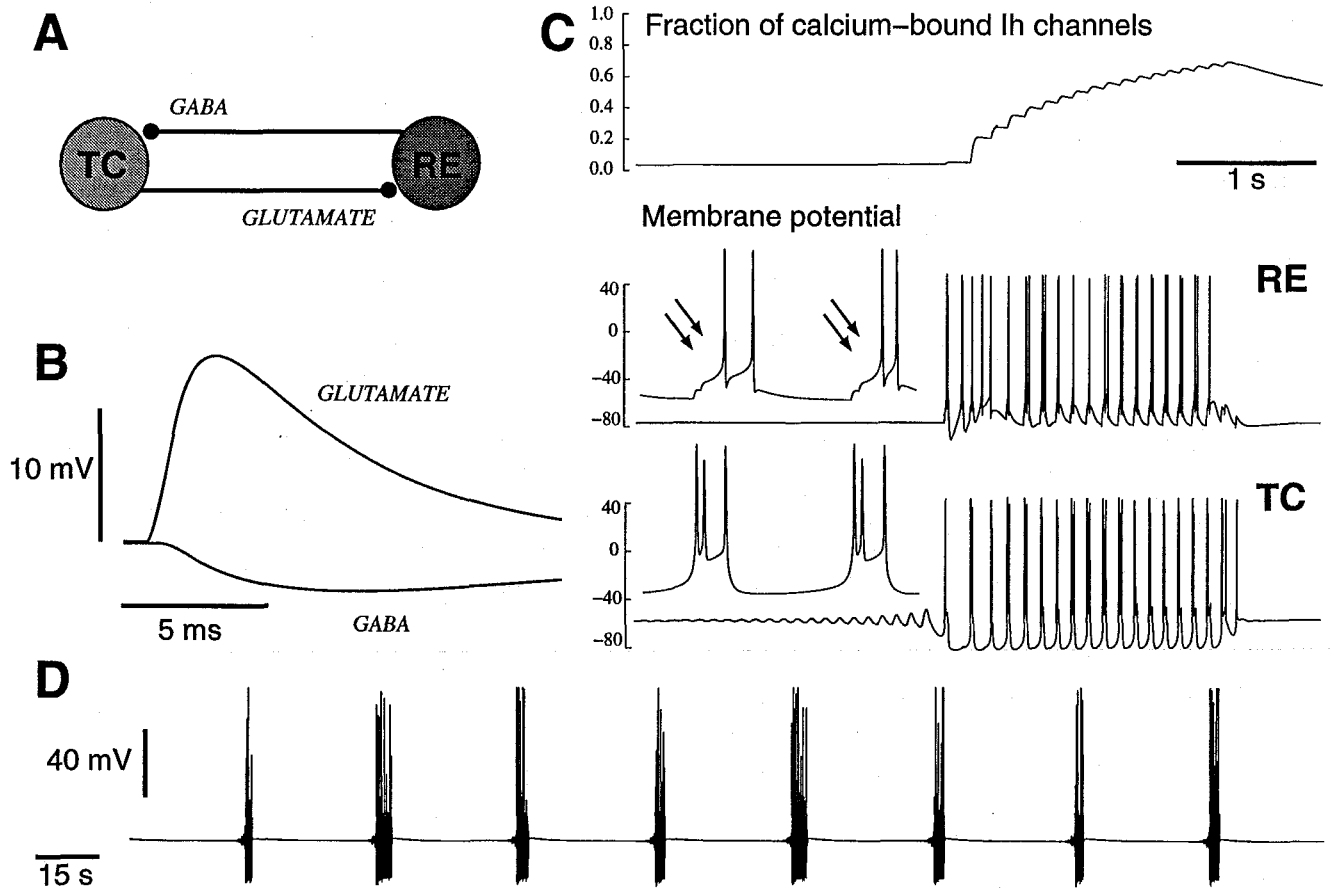


Figure 7:

Model of 8-10 Hz spindling in a pair of interconnected TC and RE cells. (A) Schematic drawing of the connections between the two types of cells. (B) Excitatory (glutamate) and inhibitory (GABA) postsynaptic potentials. (C) Sequence of spindle oscillations obtained from the interacting TC and a RE cell. The fraction of  $I_h$  channels bound to intracellular  $Ca^{2+}$  and the membrane potential of RE and TC cells are shown from top to bottom. For each cell, an inset shows two bursts at higher temporal resolution (magnification  $\times 10$ ). EPSPs on the RE cell are indicated by arrows. D. Sequences of spindles in the TC cell from the same model on a longer time scale. Modified from Destexhe et al., 1993b.

which activated  $I_T$  in the RE cell. The RE cell started bursting at 8-10  $Hz$  and entrained the TC cell to this oscillation, but the feedback of the TC cell was necessary to maintain the 8-10  $Hz$  rhythmicity. This was supported by another modeling study showing that TC cells were unable to generate oscillations in the 8-10  $Hz$  range without the help of EPSPs/IPSPs from other structures (Lytton et al., 1996b).

In the TC-RE circuit, at each cycle of the oscillation,  $Ca^{2+}$  bound to the  $I_h$  channels in the TC cell and shifted the voltage activation curve for  $I_h$ , leading to the cessation of oscillations in a manner similar to the waxing-and-waning slow oscillations in isolated TC cells.

This 2-cell model reproduced many of the properties of spindle oscillations observed in slices (von Krosigk et al., 1993; Bal et al., 1995a, 1995b). In particular, block of GABA<sub>A</sub> receptors by application of bicuculline transformed the spindle behavior by slowing down the frequency to 2-4  $Hz$  (von Krosigk et al., 1993). Further application of a GABA<sub>B</sub> receptor antagonist abolished these slowed oscillations, indicating that they were mediated by GABA<sub>B</sub> IPSPs. We could reproduce the slow synchronized oscillations in the model by either slowing down the decay time of a single GABAergic current (Destexhe et al., 1993b) or by blocking of the GABA<sub>A</sub> current when both GABA<sub>A</sub> and GABA<sub>B</sub> receptors were modeled in the RE-to-TC interaction (see Section 7).

However, blocking all GABAergic conductances does not lead to the cessation of oscillatory activity in this model because the TC cell needs to have spontaneous oscillatory activity: this may be relaxed in models of larger networks where there is a range of intrinsic properties among the TC cells, as observed *in vitro* (Leresche et al., 1991). There could be differences in the resting membrane potentials of the cells, as would occur if they had different values of  $I_h$  conductance, as we suggest. Even if most of TC cells are in a "relay" mode, with a depolarized resting membrane potential around -60  $mV$ , some TC cells could oscillate spontaneously due to a reduced  $I_h$  maximal conductance. This is consistent with current-clamp recordings in TC cells *in vitro* (McCormick and Pape, 1990b; Leresche et al., 1991; Soltesz et al., 1991), in which both resting and spontaneously oscillating TC were found. Such an inhomogeneity of the properties of TC cells may account for the initiation and propagation of spindle activity, as shown below.

In Fig. 8, a simple circuit of two TC and two RE cells are shown. The two TC cells have different parameters. The "initiator" cell (TC1 in Fig. 8) induced rhythmicity in the otherwise quiescent circuit. The oscillation could also be started by extrinsic mechanisms such as external stimulation of any TC or RE cell in the system (not shown). The resting TC cell (TC2 in Fig. 8) acted as a conditional oscillator: although it did not oscillate spontaneously,  $I_T$  and  $I_h$  were still present in the cell and it was able to participate in oscillatory behavior.

The spontaneously oscillating TC cell (TC1 in Fig. 8) started oscillating and recruited the two RE cells, which in turn recruited the resting TC cell (TC2). The oscillation in the whole system was maintained at a frequency of 6-9  $Hz$  during the spindle. After a few cycles, the  $Ca^{2+}$ -induced augmentation of  $I_h$  conductance depolarized the membrane in both TC cells and the oscillation stopped. After a silent period of 10-20  $s$ , the spontaneously oscillating TC cell started to oscillate and the cycle repeated.

The phase relationships between the TC and RE cells could be used to assess causal relationships. In Fig. 8, the initiator TC cell (TC1) started oscillating first and entrained both RE cells. However, the other TC cell always started spindling with an IPSP and followed the RE cells. If follower TC cells constituted the majority of the TC population, then comparing RE cells with this type of TC cell could lead to the misleading interpretation that RE cells start spindle oscillations. The model therefore suggests that, even if the overwhelming majority of TC cells start spindles with IPSPs, the spindle sequence can still be initiated by a small minority of initiator TC cells.

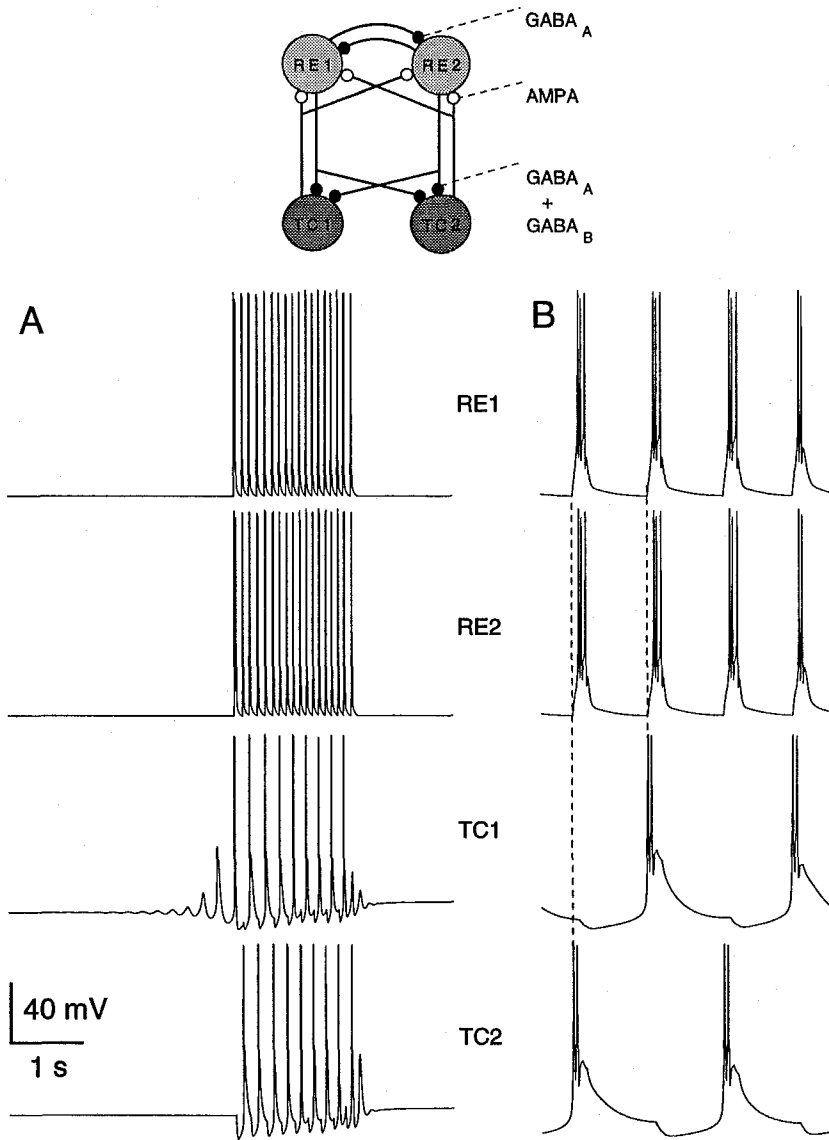


Figure 8:

Spindle oscillations in a four-neuron network of two thalamocortical and two thalamic reticular cells, connected as shown in the top diagram. One TC cell (TC1) spontaneously oscillated (initiator cell) and the second TC cell (TC2) was in a resting mode; the two RE cells were identical. Synaptic currents were mediated by AMPA/kainate receptors (from TC to RE), both GABA<sub>A</sub> and GABA<sub>B</sub> receptors (from RE to TC) and only GABA<sub>A</sub> receptors (between RE cells). A. Spindle oscillations arose as the first TC cell (TC1) started to oscillate, recruiting the two RE cells, which in turn recruited the second TC cell. The oscillation was maintained for a few cycles but died out and was repeated after a silent period of 10-20 s. B. Initial bursts of the same cells shown at 10 times higher time resolution. Modified from Destexhe et al. (1996a).

Burst firing patterns are another characteristic property of spindle oscillation. As seen in Fig. 8, the RE cells oscillated at a frequency close to 10 Hz, whereas the TC cells burst rhythmically at a lower frequency, around 5 Hz. This "intermittent bursting" phenomenon is observed in intracellular recordings of TC cells during spindle oscillations (Andersen and Andersson, 1968; Steriade and Llinás, 1988; Muhlethaler and Serafin, 1990; von Krosigk et al., 1993; Bal et al., 1995a). The mechanism underlying intermittent bursting was described in a model based on the presence of  $I_h$  (Kopell and LeMasson, 1994) and the same mechanism applies to TC neurons (Wang, 1994; Wang et al., 1995). We observed the same phenomenon in the 4-neuron model when the strength of GABAergic (RE to TC) conductances was strong conductances, and each IPSP was powerful enough to elicit a rebound bursts. In this case, spindling could be generated with only a single pair of TC and RE cells (Fig. 7). For weaker inhibitory conductances, not all IPSPs may evoke rebound bursts, with the consequence that at least two cells of each type are needed in a minimal model of spindling (Fig. 8).

*In vitro* experiments show that blocking TC-RE synaptic interconnections suppresses oscillatory behavior in both TC and RE cells (von Krosigk et al., 1993; Bal et al., 1995a, 1995b). The present model is compatible with this result if resting TC cells are typical of the majority of the TC population. After blocking all synaptic receptors, only the few spontaneously oscillating TC cells will continue to oscillate, but all other TC cells and RE cells will remain silent.

This model of interaction between two TC cells and two RE cells can be scaled up to larger networks. In Fig. 9, a model with 50 TC and 50 RE cells is shown having the same types of cells and synaptic receptors as in Fig. 8. Only one spontaneously oscillating TC cell was present (TC1) and all other TC cells were in a resting, or relay mode, but all the RE cells were identical. The behavior of the 100-cell network was similar to that observed in the 4-cell network: the "initiator" TC cell (TC1 in Fig. 9) started oscillating spontaneously and recruited neighboring RE cells, which in turn recruited other TC cells, which recruited additional RE cells at the next cycle, etc. These progressive to-and-fro interactions between cells in the TC and the RE layers recruited additional cells into the spindle oscillation on every cycle through lateral interactions. The whole system oscillated at a frequency of 8-10 Hz. After a few cycles, the  $Ca^{2+}$ -induced augmentation of  $I_h$  conductance in TC cells stopping the oscillation. After a silent period of 10-20 s, the spontaneously oscillating cell started to oscillate again and the cycle repeated.

Although the 100-cell network contained mechanisms identical to those used in the 4-cell network, the topographically restricted connectivity between the TC and RE layers supported additional propagating wave phenomena. Qualitatively similar behavior was observed with different sets of parameters as long as the connectivity was topographically organized (not shown). The model therefore suggests that this type of local connectivity is critical for propagating phenomena. At each cycle of the oscillation, a larger pool of either TC or RE cells were recruited in the spindle oscillation. This suggests that the propagation velocity may reflect the number of cells recruited at every cycle, and therefore should be a function of the divergence of the connectivity, and the ability of one cell to fire another.

The spatiotemporal portrait of these oscillations is shown in Fig. 10. During the oscillation, groups of cells segregated into localized clusters of activity that discharged in alternation. This phenomenon was related to the subharmonic bursting properties of TC cells which do not allow the whole network to fire in unison at around 10 Hz. Individual clusters of activity also propagated with the same velocity as the whole oscillation. The spindles in the model were composed of a series of successive clusters of activity that followed each other and propagated through the TC-RE network. The cluster of activity constituting the front of the oscillation can be seen clearly from the top series

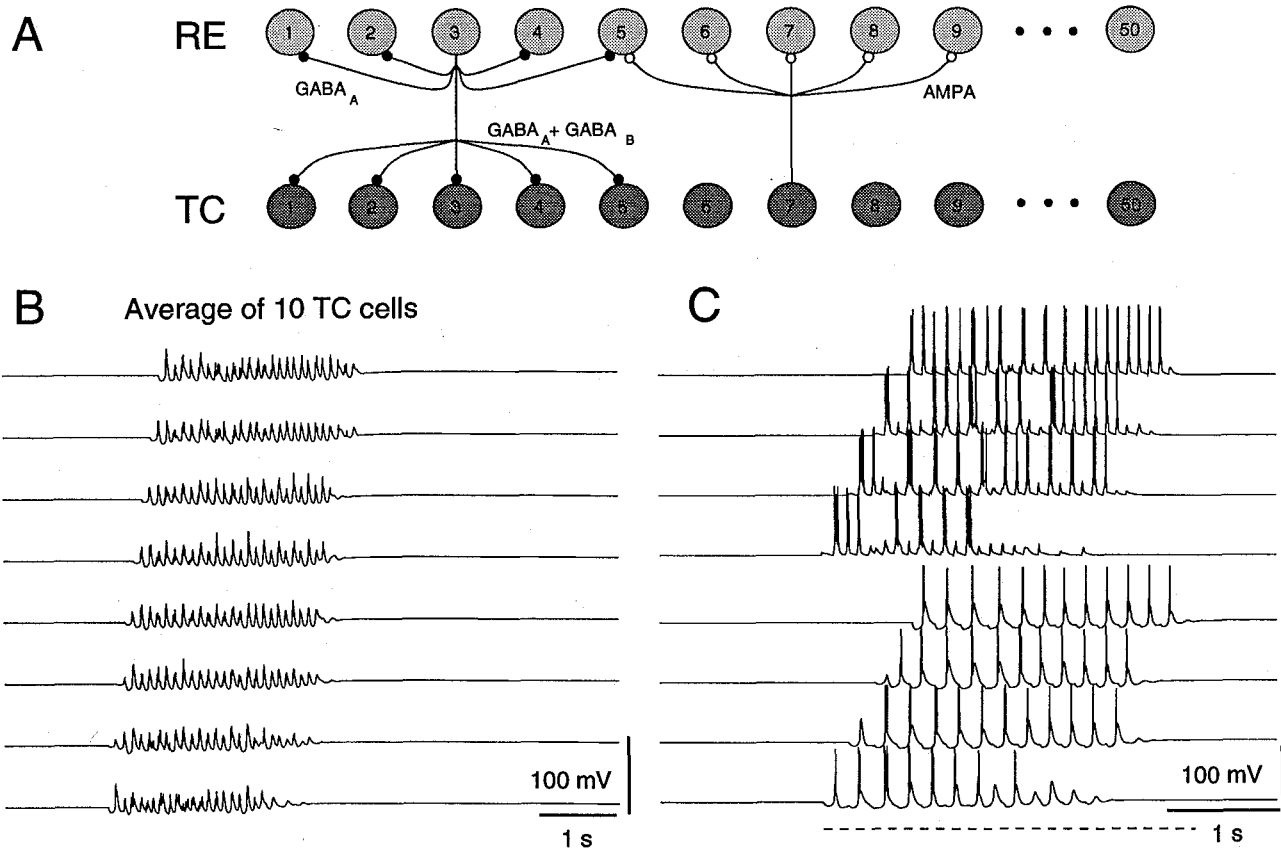


Figure 9:

Spindle oscillations in a network of 50 thalamocortical and 50 thalamic reticular cells. A. Diagram of connectivity between TC and RE cells with localized axonal projections. Axons from TC cells ramified in the RE nucleus and contacted a local patch of 5 RE cells (10% of the RE cells in the network). Axons from RE cells contacted TC cells with the same fan-out and also had collaterals onto neighboring RE cells. The connectivity was translationally invariant, so each cell had the same projections as the representative ones shown here. TC1 was a spontaneously oscillating cell, whereas all other TC cells were in resting mode. B. Spindle oscillations at various sites of the network. Averaged membrane potentials were computed from 10 neighboring TC cells taken at 8 equally spaced sites. C. Membrane potential of 4 TC (4 bottom traces) and 4 RE cells (upper traces) from the same simulation as in B (Cells 10,20,30,40). The propagating waves in these simulations were similar to those observed *in vitro* (Kim et al., 1995). Modified from Destexhe et al. (1996a).

of frames in Fig. 10.

The waxing-and-waning of the spindle oscillation in the model is caused by factors intrinsic to the TC cells. The ability of the RE cell to fire the TC cell gradually diminished, until oscillations could no longer be sustained. In our model, the primary factor for the waning was the binding of intracellular  $Ca^{2+}$  to  $I_h$ , which progressively augmented the  $I_h$  conductance on each cycle, until the TC cell failed to oscillate. This is consistent with the increase of conductance observed in TC cells at the end of the spindle oscillation (Bal and McCormick, 1995; Nuñez et al., 1992).

Progressive recruitment between TC and RE cells was also observed in other thalamic models based on different types of kinetics for the ionic currents (Golomb et al., 1994; Wang et al., 1995; Golomb et al., 1996). In these models, there was no mechanism included to produce the waxing-and-waning seen in thalamic spindles, so the TC-RE oscillations were sustained. However, the leading edge of the traveling waves in their model had properties that were quite similar to those observed in the more detailed model presented here, suggesting that some general properties may be robust. They also analyzed the influence of the connectivity between the TC and RE cells in this model (Golomb et al., 1996) and concluded that the localized axonal projections could account for the propagation velocities of spindle oscillations, in agreement with the model shown in Fig. 9.

The results of modeling thalamic oscillations are entirely consistent with *in vivo* and *in vitro* recordings of spindle oscillations in different preparations. They also account for the pharmacological properties of spindle oscillations as determined from thalamic slices (von Krosigk et al., 1993). In particular, the models and experiments support the hypothesis that the kinetics of intrinsic currents and synaptic receptors present in the TC-RE loop generate waxing-and-waning spindle oscillations.

The models also suggest that spindle oscillations critically depend on the presence of robust bursting properties in both TC and RE cells, as well as on the integrity of the synaptic connections between them. However, the observation of spindle rhythmicity in the deafferented RE nucleus *in vivo* (Steriade et al., 1987) is contrasting with this view. We show in the next section how modeling can be used to test a plausible way to reconcile these observations.

## 6 SPINDLE RHYTHMICITY IN THE ISOLATED RE NUCLEUS

Experiments in cats *in vivo* have shown that cortically-projecting thalamic nuclei lose their ability to generate spindle oscillations if they are deprived of input from the reticular thalamic (RE) neurons (Steriade et al. 1985) and that the RE nucleus can itself generate spindle rhythmicity if it is severed from thalamic and cortical afferents (Steriade et al. 1987). However, *in vitro* recordings show that slices of the RE nucleus devoid of connections with TC cells do not oscillate spontaneously (Avanzini et al., 1989; von Krosigk et al., 1993; Huguenard and Prince, 1994b; Warren et al., 1994; Bal et al., 1995b). In thalamic slices containing interconnected TC and RE nuclei, spindle oscillations are suppressed in both types of neurons if their interconnections are either physically cut, or inactivated by application of antagonists (von Krosigk et al., 1993; Bal et al., 1995a, 1995b).

How can these apparently contradictory experimental results be reconciled? Is it possible that a network of RE cells interconnected with mutually inhibitory synapses may produce oscillations similar to those observed *in vivo*? We first investigated a simple system of two interconnected RE neurons, then extended the model to two-dimensional networks of RE cells. The synaptic currents were based on kinetic models of the postsynaptic receptors (Destexhe et al., 1994d) that were similar to those presented in the previous section.

A simple circuit that consists of a pair of interconnected RE cells with GABA<sub>A</sub> synapses is shown in Fig. 11. The interconnections were mediated by GABA<sub>A</sub> receptors, in agreement with

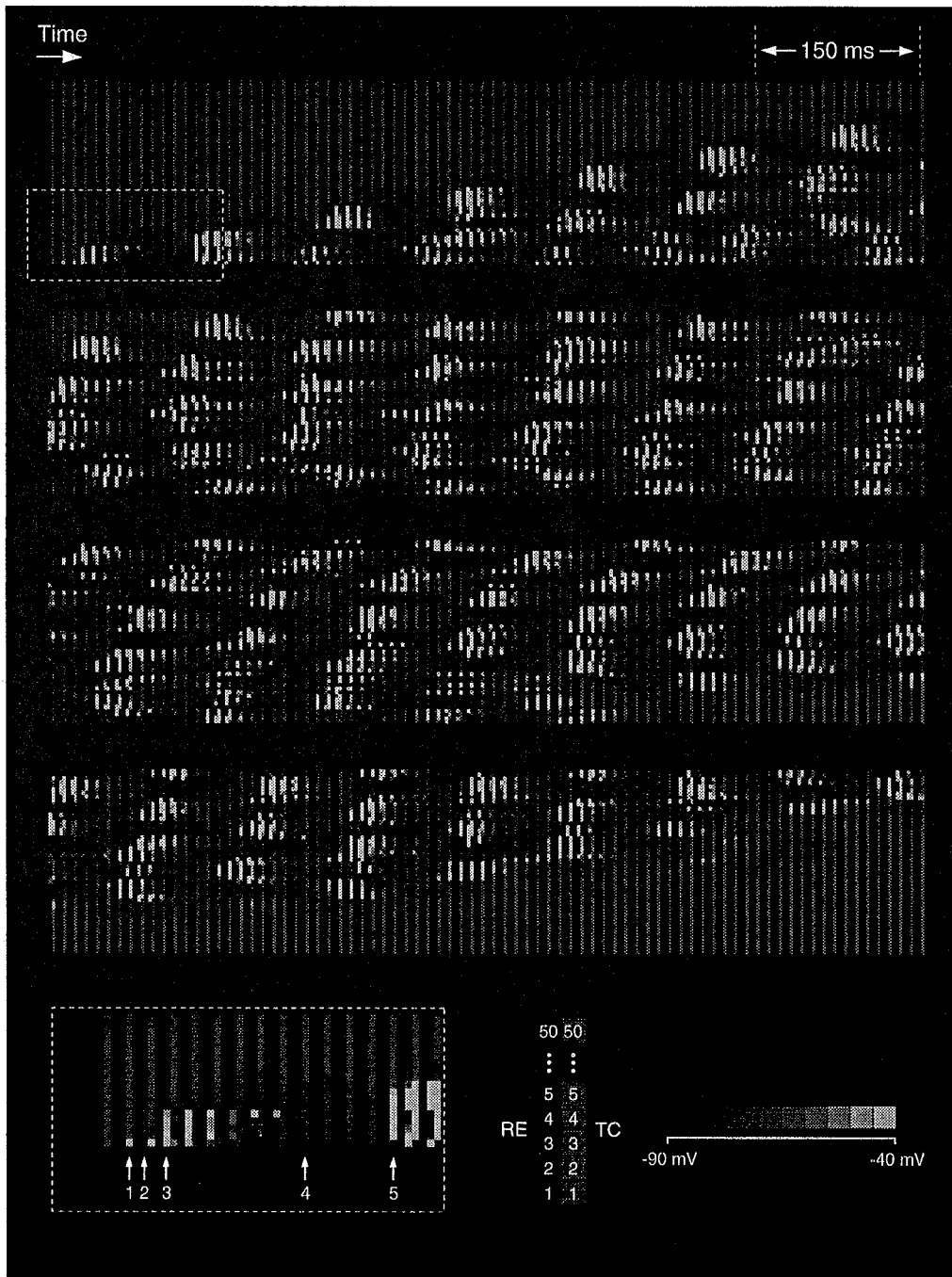


Figure 10:

Spatial patterns of burst discharges during spindle oscillations in the 100-cell network model. The spatial activity of the network is represented as a series of snapshots of activity. A series of successive frames is shown for an entire spindle sequence (320 frames with 10 ms between frames; sequence indicated by a dashed line in Fig. 9B-C). The activity consisted of a series of distinct clusters of activity propagating in the same direction. The initiation of the spindle sequence is expanded on bottom left. For each snapshot, 50 TC and 50 RE cells were displayed vertically as indicated (middle scheme at bottom). The value of the membrane potential for each neuron was coded using a color scale ranging in 10 steps from -90 mV (blue) to -40 mV (yellow). Modified from Destexhe et al. (1996a).

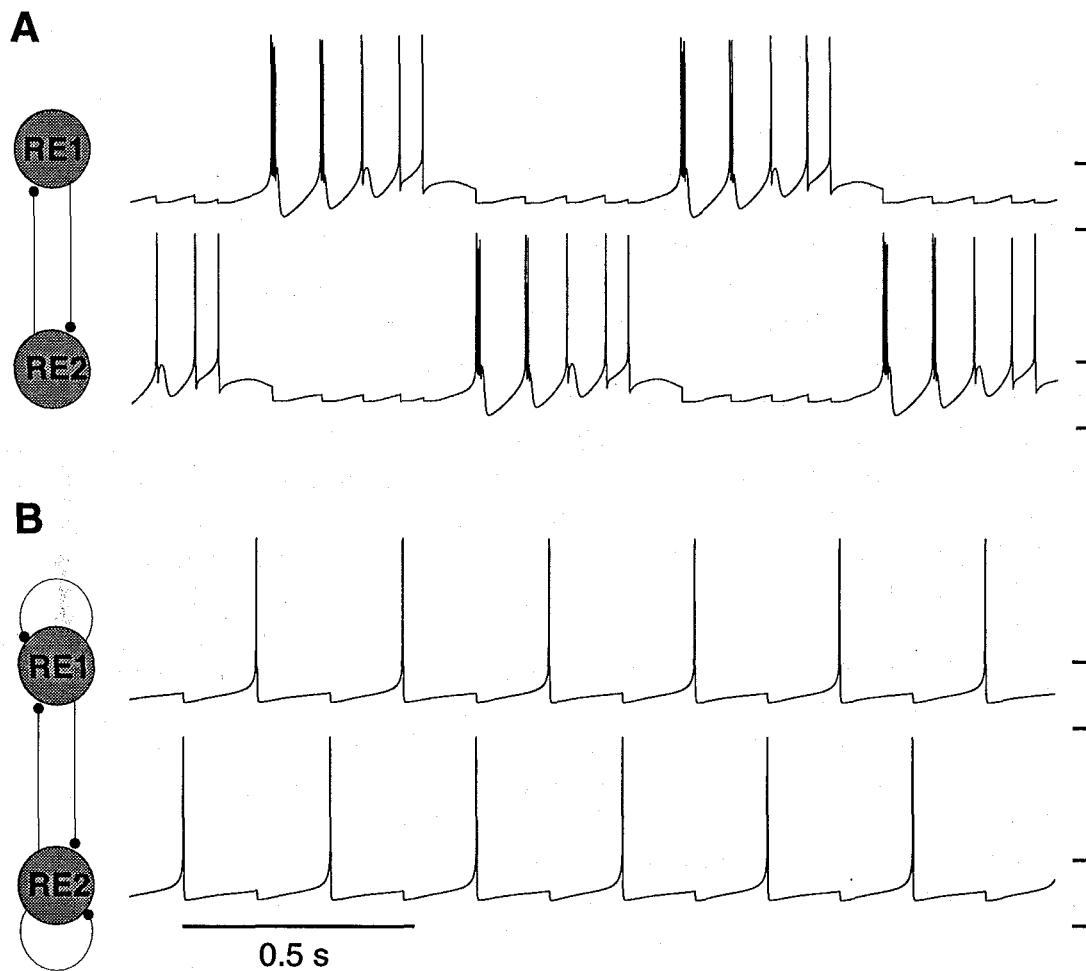


Figure 11:

Two interconnected RE cells are capable of sustained oscillations although they do not oscillate individually. Two single-compartment RE neurons (as in Fig. 5) were interconnected with GABA<sub>A</sub> synapses. The diagram of connectivity is shown on the left and traces from simulations of the two neurons are shown on the right. (A) Reciprocal interactions produced oscillations in which a sequence of rhythmic bursts are alternating in the two cells. (B) The addition of self inhibitory connections produced more synchronized oscillations. Vertical calibration bars are from -100 to -50 mV. Modified from Destexhe et al., 1994a.

a number of electrophysiological studies (McCormick and Prince, 1986; Spreafico et al., 1988; Bal and McCormick, 1993; Destexhe et al., 1994a; Bal et al., 1995b). This two-neuron system displayed spontaneous oscillations if the GABAergic conductances were sufficiently strong. If self-connections were included, the two RE neurons oscillated synchronously in the 6-9 Hz range, with one neuron firing every two cycles.

We also investigated the dynamics of a system of 100 RE neurons organized in a two-dimensional array with local connectivity, a better approximation to the organization of the RE than full connectivity. "Dense proximal connectivity" was used, in which each neuron projected to all other neurons within some radius, as shown in Fig. 12A. The activity in the network with fan-ins from and fan-outs to 25 neighboring neurons showed a complex, oscillatory dynamics at a frequency of 6.5-9 Hz (Fig. 12B-C). Analysis of the snapshots of activity of the network revealed a 6.5-9 Hz subthreshold oscillation which was the major oscillatory component of the average membrane poten-

tial. In addition, the average membrane potential displayed alternating periods of synchronized and desynchronized activity (Fig. 12C), reminiscent of the waxing-and-waning field potentials recorded in the isolated RE *in vivo* (Steriade et al., 1987). During these waxing-and-waning fluctuations of amplitude, the activity of neurons in the network alternated between periods of coherent oscillatory activity, characterized by well defined propagating waves, and periods of less coherent activity, in which the patterns of spatiotemporal activity were less well organized (Fig. 12B).

Networks of inhibitory neurons exhibiting post-inhibitory rebound have been used to model central pattern generators in motor systems (Perkel and Mulloney 1974; Rowat and Selverston, 1993). Previous models of the RE nucleus have used synaptic interactions described by sigmoid-type of coupling, which assumed a smooth transformation between the presynaptic voltage and the postsynaptic conductance in the synapse (Destexhe and Babloyantz, 1992; Wang and Rinzal, 1992, 1993). One of these models (Wang and Rinzal, 1992, 1993) demonstrated the presence of synchronized oscillations if the decay of the synaptic current was sufficiently slow. Another model (Destexhe and Babloyantz, 1992) showed that synchronized rhythms could be observed if the connectivity between neurons were not restricted to immediate neighbors, but rather to a more extended population of neighboring cells. Similar oscillatory states were also reported from other network models (Golomb and Rinzal, 1994; Golomb et al., 1994). However, the oscillations in these models have global synchrony and are quite different from the oscillations observed in the average membrane potential from the model described above (Destexhe and al., 1994a). In the latter model, fluctuations of the phase relationships between individual neurons gave rise to waxing-and-waning average activities, similar to the type of spindle rhythmicity observed in the isolated RE nucleus *in vivo* (Steriade et al., 1987).

We have shown that the same model can predict both TC-RE spindling activity and spindle rhythmicity in the isolated RE nucleus. However, an explanation is still needed for why the isolated RE does not show spontaneous oscillations *in vitro* (Avanzini et al, 1989; von Krosigk et al., 1993; Huguenard and Prince, 1994b; Warren et al., 1994; Bal et al., 1995b). A possible explanation for these discrepancies is based on the effect of neuromodulators on RE cells (Destexhe et al., 1994b).

In Fig. 6, we illustrate how neuromodulators, such as NE and 5HT, can control the level of the membrane potential in RE cells. Starting with the RE network model described above, we assumed that the leak  $K^+$  current was controlled by 5 NE/5HT synapses in each cell, as in Fig. 6. When the level of NE/5HT activity was 20%, the resting membrane potential of the RE cells (Fig. 13) had the same behavior as for the simulations shown previously (Fig. 12). However, if this noradrenergic/serotonergic input is suppressed, the network no longer sustained oscillations (Fig. 13).

The sensitivity of the oscillations to the membrane potential depended on the relative values of the resting level and the chloride reversal potential  $E_{Cl}$  (which provided the driving force for the GABA<sub>A</sub> receptors). If the resting level was too close to  $E_{Cl}$ , the resulting shunting inhibition failed to trigger a rebound burst in the RE cell. However, if the resting level was maintained higher, for example through the action of neuromodulators, then the driving force of the IPSPs could trigger LTSs in RE cells and the network then showed sustained oscillations.

This interpretation is supported by data showing that the resting membrane potential of RE cells *in vitro* is relatively hyperpolarized ( $-71.2 \pm 6.0$  mV in Huguenard and Prince, 1994b). Another consistent piece of evidence is that under various anesthetics for which spontaneous oscillations were reported in the isolated RE *in vivo* (Steriade et al., 1987), the resting membrane potential of cat RE cells was relatively depolarized ( $-63.8 \pm 1.2$  mV in Contreras et al., 1993).

Thus, the presence of a weak neuromodulatory drive may explain why the isolated RE nucleus oscillates *in vivo* but not *in vitro*. The model predicts that spontaneous sustained oscillations could be observed in slices of the RE nucleus if the resting level of RE cells could be brought to more

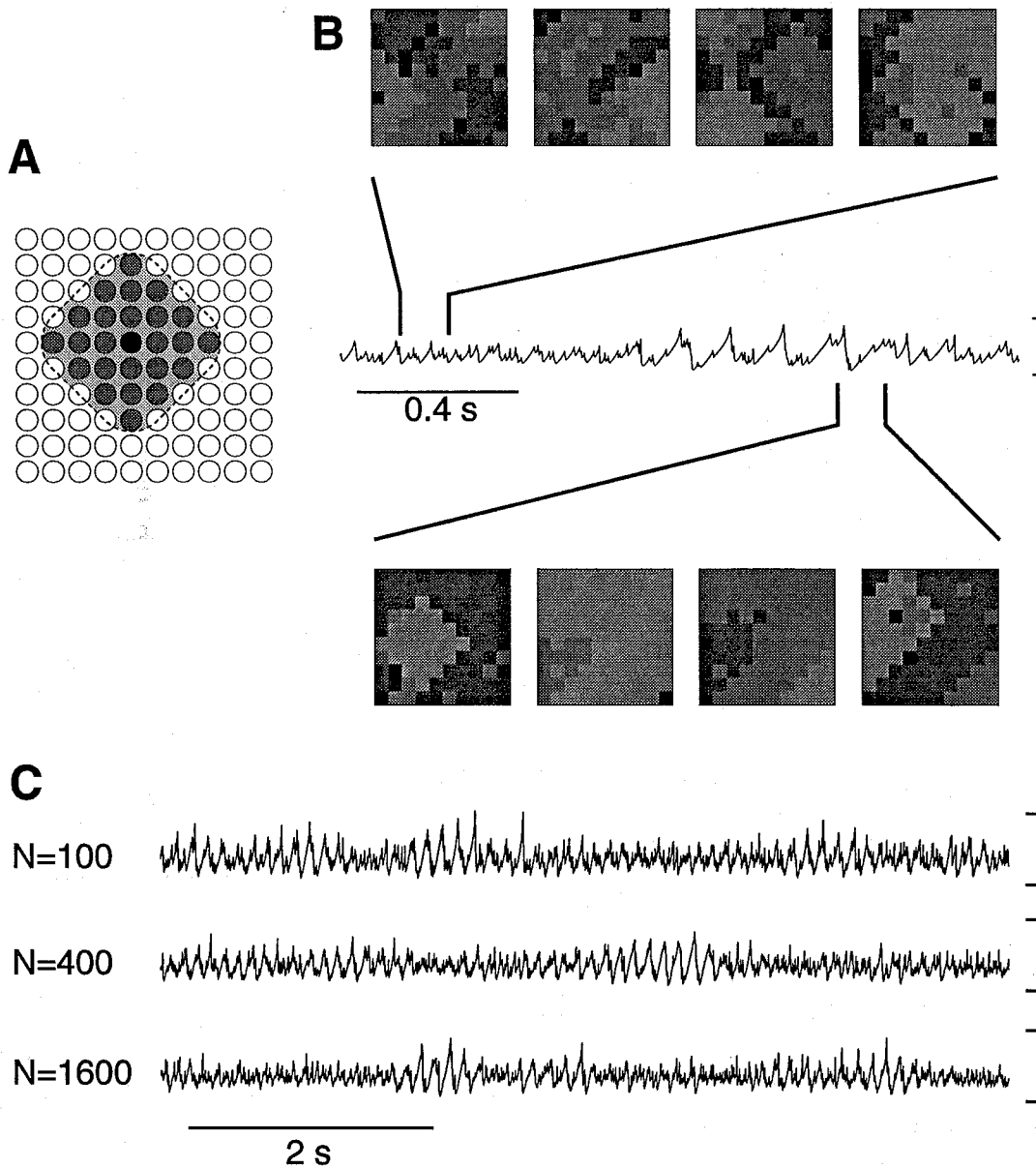


Figure 12:

Three networks with 100, 400 and 1600 interconnected RE cells show population rhythmicity with waxing-and-waning amplitude fluctuations. (A) Pattern of connectivity: a given RE neuron (black) connected with 24 other RE cells (dark gray) and itself. (B) Snapshots of activity in a 100 neuron network shown with the average membrane potential. Each square frame represents a snapshot of the 100 RE neurons, arranged in a 10 x 10 array. The value of the membrane potential for each neuron is shown as a gray scale ranging in 10 steps from -90 mV (white) to -60 mV (black). Membrane potentials higher than -60 mV are shown in black. The time step between frames is 40 ms. (C) Average membrane potentials for networks with  $N = 100$ ,  $N = 400$  and  $N = 1600$  neurons. For  $N = 400$  and  $N = 1600$ , the local average membrane potential was obtained by averaging over a disk of 113 neurons in the center of the network. Vertical calibration bars for the average membrane potential traces are from -80 mV to -70 mV. Modified from Destexhe et al., 1994a.

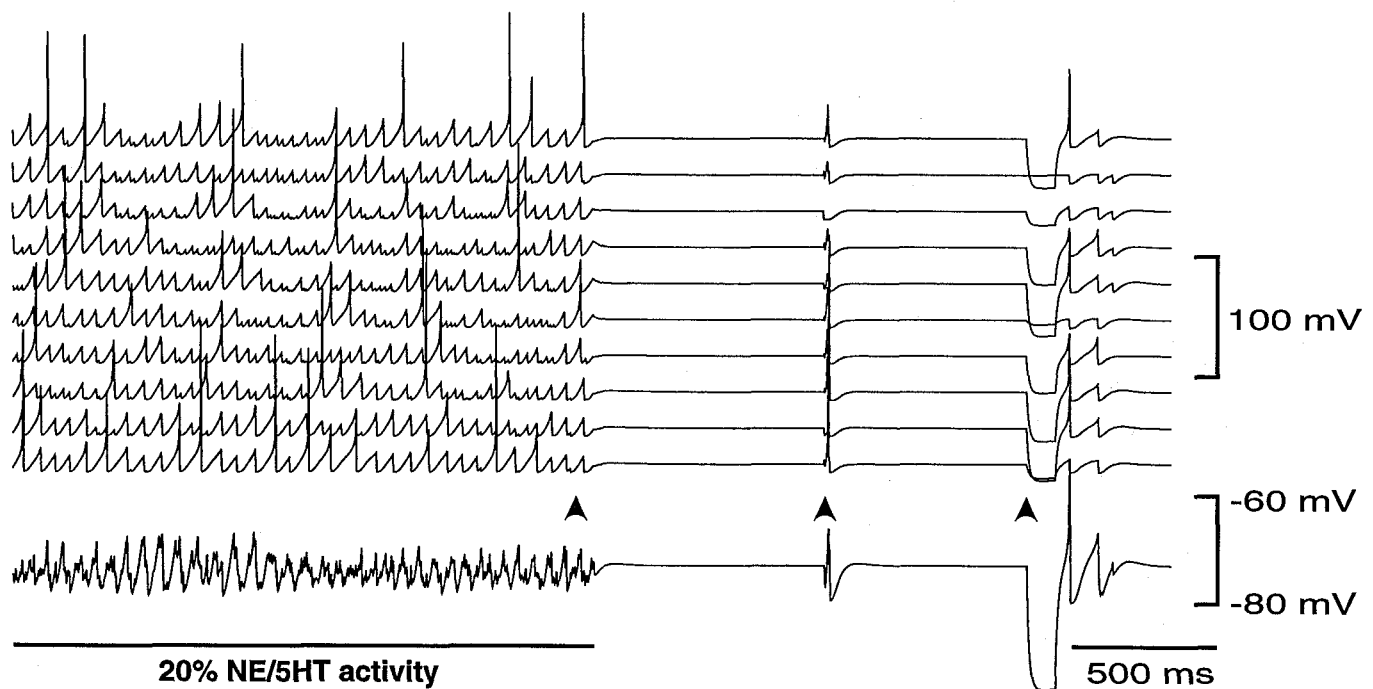


Figure 13:

Oscillations in a model of the isolated RE nucleus are sensitive to the membrane potential. The network model of 100 RE cells was similar to that shown in Fig. 12. The top 10 traces represent the activity of 10 neurons in the network and the bottom trace is their average membrane potential. 20% of NE/5HT synapses were initially activated (as in Fig. 6). In this condition, the network showed self-sustained oscillations at a frequency of 10-16 *Hz* and the average membrane potential displayed waxing-and-waning fluctuations of amplitude. After 2 seconds (first arrow), all NE/5HT synaptic activity was suppressed; the resulting hyperpolarization prevented the network from sustaining oscillations. Depolarizing (second arrow) or hyperpolarizing (third arrow) current pulses injected simultaneously in all neurons (with random amplitude) could not restore spontaneous oscillations. The latter condition might correspond to the membrane potential of RE cells *in vitro*. Modified from Destexhe et al., 1994b.

depolarized values. This could be achieved by bath application of NE/5HT agonists in weak concentration to depolarize all RE neurons to the -60 to -70 *mV* range. Another prediction is that NE/5HT antagonists should suppress oscillatory behavior in the isolated RE nucleus *in vivo*. The same results should also be found in other models of networks of inhibitory neurons displaying rebound bursts (Wang and Rinzel, 1993; Golomb et al., 1994).

## 7 PAROXYSMAL DISCHARGES IN THE THALAMUS

Clinical, electrophysiological and pharmacological studies suggest that some types of generalized epilepsy could be a perversion of spindle oscillations (see Avoli et al., 1990 for a review; see also Steriade et al., 1993a). Antagonists of the GABA<sub>B</sub> receptor have been effective in preventing the development of spike-and-wave discharges in some animal models (Hosford et al., 1992; Liu et al., 1992), suggesting that GABA<sub>B</sub> receptors are critically involved in the cellular mechanisms of this rhythmicity. This hypothesis was further supported by experiments in ferret thalamic slices in which the application of GABA<sub>A</sub> antagonists transformed the spindle oscillations into slower and more synchronized oscillations (von Krosigk et al., 1993), which were abolished by GABA<sub>B</sub> antagonists. Although these studies are compatible with the possibility of an intrathalamic GABA<sub>B</sub>-mediated site underlying generalized epileptic discharges, the mechanisms that generate these paroxysmal patterns are still uncertain.

Additional evidence may be found at the cellular level. Both TC and RE neurons display prolonged burst discharges following application of convulsants *in vitro* (Soltesz and Crunelli, 1992; von Krosigk et al., 1993; Huguenard and Prince, 1994a, 1994b; Bal et al., 1995a). On the other hand, reinforcing the lateral inhibition in the RE nucleus tends to diminish the occurrence of burst discharges, and has been proposed as a mechanism of action of anti-absence drugs, such as clonazepam (Huguenard and Prince, 1994a). We have used the thalamic slice model to test possible mechanisms for the genesis of these abnormal discharges.

The first step was to obtain an accurate model of GABA<sub>B</sub> currents. In general, strong stimuli are needed to activate GABA<sub>B</sub> responses, both in hippocampal (Dutar and Nicoll, 1988; Davies et al., 1990) and thalamic slices (Soltesz and Crunelli, 1992). When stimulating the RE nucleus, biphasic (GABA<sub>A</sub> and GABA<sub>B</sub>) IPSPs are evoked in TC cells, and the ratio between peak GABA<sub>A</sub> and GABA<sub>B</sub> currents evoked by RE neurons is insensitive to the intensity of the stimulation (Huguenard and Prince, 1994b) but changes markedly if the discharge of RE cells is enhanced by pharmacological means (Huguenard and Prince, 1994a, 1994b; Bal et al., 1995a; Sánchez-Vives et al., 1995).

We recently reproduced the typical features of GABA<sub>B</sub> responses based on a kinetic model of the G-protein transduction underlying the activation of K<sup>+</sup> channels (Destexhe and Sejnowski, 1995) under the assumption that the independent binding of several G-protein subunits were needed to activate these K<sup>+</sup> channels. In the model, a strong stimulus is needed to activate detectable GABA<sub>B</sub>-mediated currents.

We simulated the properties of GABAergic responses in thalamic slices using the bursting model of RE cells described above (Fig. 14A). Under normal conditions, stimulation of the RE nucleus evoked biphasic IPSPs in TC cells, with a rather small GABA<sub>B</sub> component (Fig. 14B). We mimicked an increase of stimulus intensity by increasing the number of RE cells discharging. The ratio between the amplitudes of the GABA<sub>A</sub> and GABA<sub>B</sub> IPSPs was independent of the intensity of stimulation, but only if the density of GABAergic synapses was low on TC cells. Blocking GABA<sub>A</sub> receptors locally in the RE nucleus enhanced the burst discharge of these cells, and evoked a more prominent GABA<sub>B</sub> component in TC cells (Fig. 14C).

Following removal of GABA<sub>A</sub>-mediated inhibition in the model (Fig. 15), the RE cells produced prolonged bursts that evoked strong GABA<sub>B</sub> currents in TC cells (as in Fig. 14C), which in turn evoked robust rebound bursts in TC cells. The mutual TC-RE recruitment entrained the system into a 3.5-4.5 Hz slow oscillation, with characteristics similar to those of bicuculline-induced oscillations observed in ferret thalamic slices (von Krosigk et al., 1993; Bal et al., 1995a, 1995b). The oscillation was produced by mechanisms similar to those previously described for spindle oscillations, but was

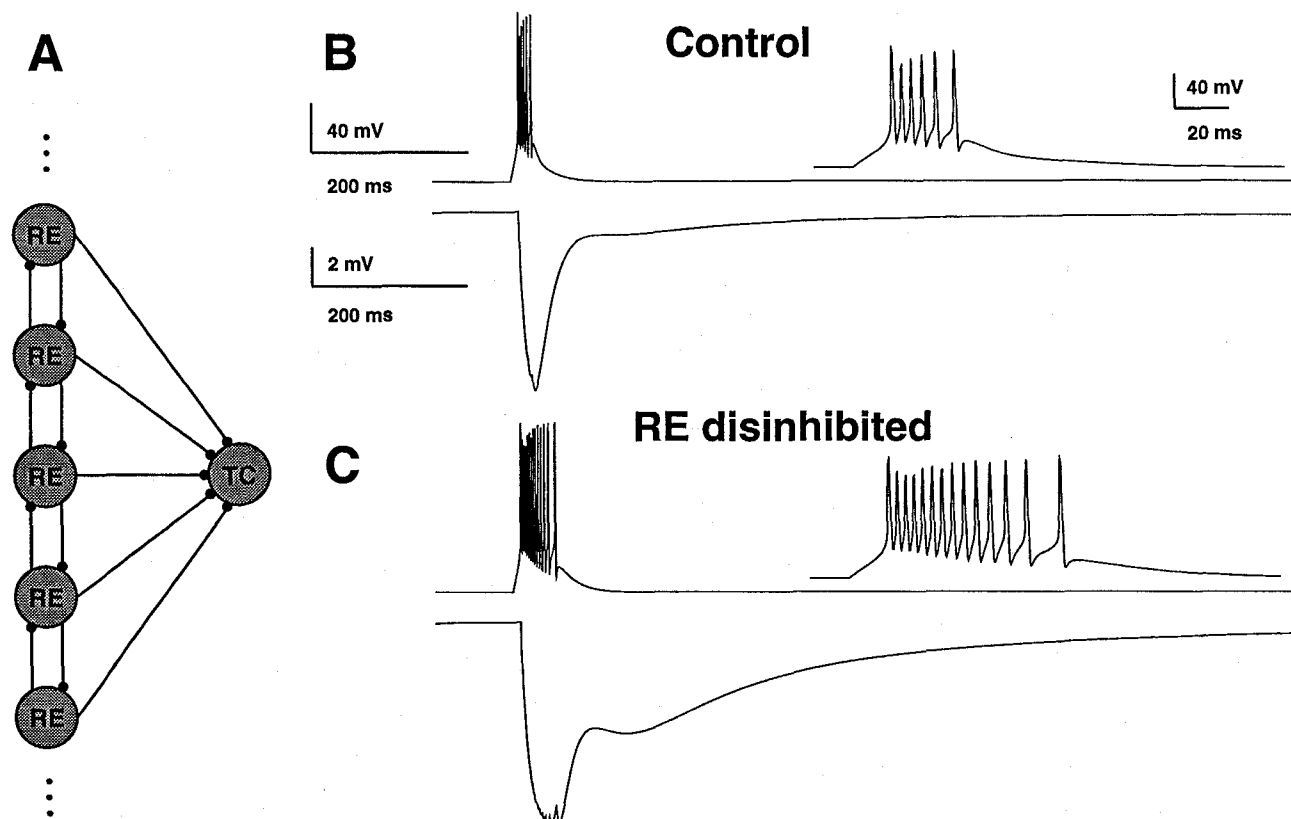


Figure 14:

Model for the enhancement of the  $GABA_B$  response in thalamocortical cells through disinhibition in the thalamic reticular nucleus. A. Connectivity of a simple network of RE cells with  $GABA_A$  receptor-mediated synaptic interactions. All RE cells projected to a single TC cell with synapses containing both  $GABA_A$  and  $GABA_B$  receptors. The TC cell had no active current in this simulation. B. In control conditions, the bursts generated in RE cells by stimulation had 2-8 spikes and evoked a  $GABA_A$ -dominated IPSP with a small  $GABA_B$  component in the TC cell (bottom trace). C. When  $GABA_A$  receptors were suppressed in RE, the bursts became prolonged and evoked a stronger  $GABA_B$  component in the TC cell. Modified from Destexhe and Sejnowski (1995).

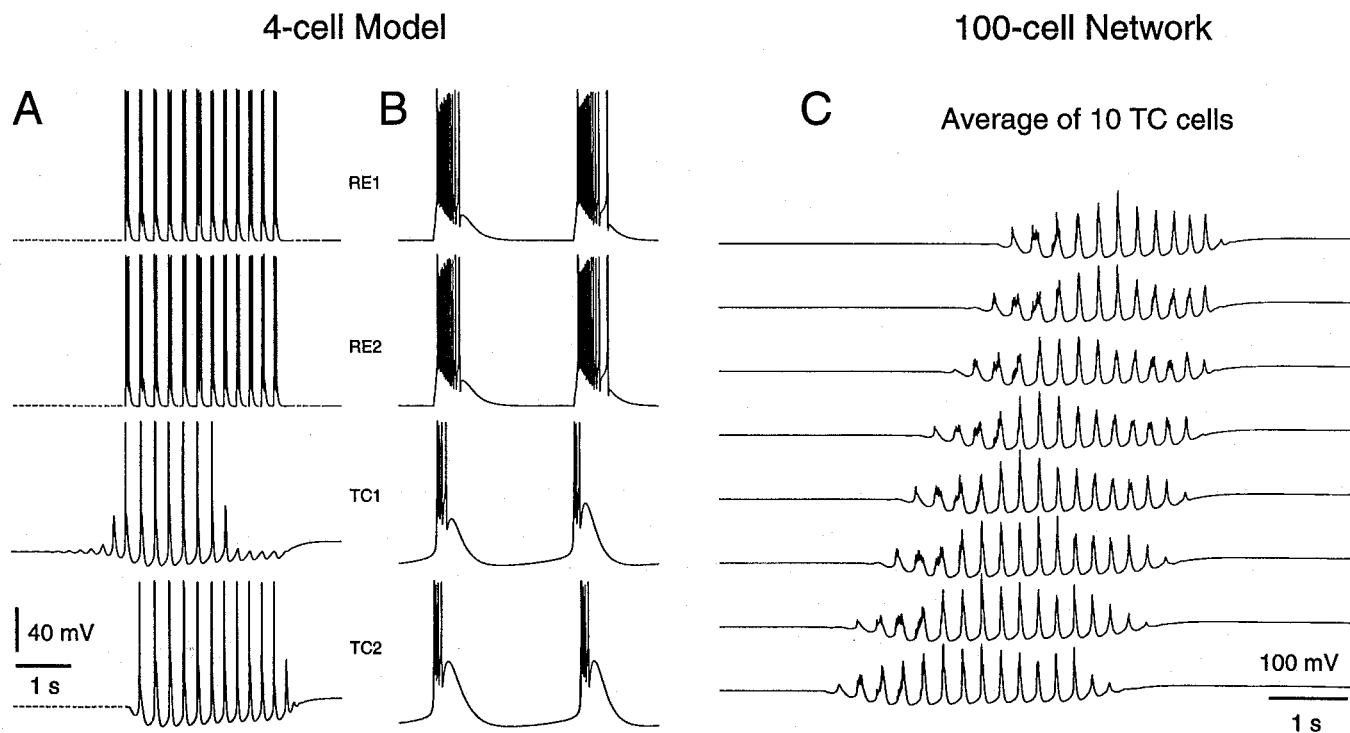


Figure 15:

A model of bicuculline-induced oscillations in coupled networks of thalamocortical and thalamic reticular cells. A. Responses from a network with two TC and two RE cells as in Fig. 8, except that all  $GABA_A$  receptors (between RE cells, and from RE to TC) were suppressed, mimicking the effect of bicuculline. A slow 3-4 Hz oscillation was obtained as the first TC cell (TC1) started to oscillate, recruiting the two RE cells, which in turn recruited the second TC cell. The oscillations were more synchronized, of slower frequency, and had a 15% longer silent period than in the model of spindle waves (Fig. 8). The bursting discharges were prolonged due to the loss of lateral inhibition in the RE. B. First bursts of the same cells shown at 10 times higher time resolution. Unlike in spindles, the two TC cells burst in phase. C. Average membrane potentials of slow bicuculline-induced oscillations in a 50 TC and 50 RE network (as in Fig. 9, with  $GABA_A$  receptors suppressed). The propagating oscillation had a slower frequency and higher degree of synchrony compared to the spindle oscillations shown in Fig. 9. Modified from Destexhe et al. (1996a).

slower and more synchronized.

The restricted topographic connectivity between the TC and RE layers supported propagating wave phenomena for the slow oscillations, which were initiated, propagated and terminated by the same mechanisms that supported spindle oscillations, except that the propagation velocity was slower and the activity was not organized in distinct clusters, but each burst tended to recruit a much larger population of cells into prolonged discharges (Destexhe et al., 1996a). Occasionally a phase shift could be observed but with no preferential direction. These properties are characteristic of bicuculline-induced oscillations in ferret thalamic slices (Kim et al., 1995).

A similar model also reproduced the increased synchrony and stronger discharges of thalamic cells following blockage of  $GABA_A$  receptors (Wang et al., 1995). However, this synchronous state in the model coexisted with a desynchronized state of the network, which has never been observed experimentally. In a subsequent model (Golomb et al., 1996), robust synchronized oscillations were obtained by using a  $GABA_B$  receptor model with cooperative activation, similarly to that in Figs. 14. This independent modeling study also reached the conclusion that the transition from spindle to paroxysmal patterns can be achieved provided there was cooperativity in  $GABA_B$  responses.

An alternative explanation has been proposed based on the disinhibition of interneurons projecting to TC cells with GABA<sub>B</sub> receptors only (Soltesz and Crunelli, 1992). A model including TC, RE and interneurons (Wallenstein, 1994b) reproduced the stronger discharges in TC cells following application of bicuculline. Although it is possible that this mechanism plays a role in thalamically-generated epileptic discharges, it does not account for the recent experiments showing the decisive influence of the RE nucleus in preparations devoid of interneurons (Huguenard and Prince, 1994a, 1994b).

## 8 DENDRITIC CURRENTS IN THALAMIC NEURONS

Thus far, we have shown that single-compartment models of thalamic neurons, provided with a minimal set of intrinsic and synaptic currents, can account for a large body of phenomena observed experimentally. Some of the finer details found in intracellular recordings from thalamic cells can be addressed in models that include more compartments. Using a multicompartment model of the RE cell, we have tested the hypothesis that  $I_T$  is localized with high densities in the dendrites, and studied the impact of dendritic  $I_T$  on the responsiveness of the cell.

The models were based on voltage-clamp and current-clamp experiments on RE cells (Destexhe et al., 1996b): (a) An RE cell was intracellularly recorded in slices and filled with biocytin (Huguenard and Prince, 1992); (b) the morphology of the cell was reconstructed using a computerized tracing system and the geometry encoded into a multicompartment model; (c) the simulations were compared directly to the recordings from the same cell and precise values of the parameters obtained for that cell; (d) more than 90% of the dendrites were removed from the model to simulate acutely dissociated cells, in which most of the dendrites are removed by the dissociation procedure.

The intact-cell and dissociated-cell models were then used to determine the precise properties of  $I_T$  in RE cells from voltage-clamp recordings. The procedure was to: (a) estimate the kinetic parameters of  $I_T$  based on recordings on dissociated cells; (b) compare the amplitude of  $I_T$  in dissociated vs. intact cells and use the model to simulate a plausible dendritic/somatic distribution of the current; (c) simulate voltage-clamp experiments and try to account for the differences between intact and dissociated cells based on dendritic  $I_T$ ; (d) analyze the fine structure of the burst; (e) and simulate sustained synaptic currents in a cell with dendritic  $I_T$  to account for the properties of these cells *in vivo* (Contreras et al., 1993).

The results obtained from this combined modeling and experimental study were as follows: (a) A Hodgkin and Huxley (1952) type model accounted for the activation and inactivation of  $I_T$  with rate constants adjusted to the values observed in dissociated RE cells (see Huguenard and Prince, 1992); (b) The peak amplitude of  $I_T$  was an order of magnitude larger in intact cells than in dissociated cells, and this behavior could be simulated by assuming high densities of  $I_T$  in the dendrites; (c) The kinetics of  $I_T$  was significantly slower in intact cells, and this property could be simulated only if the major portion of  $I_T$  was located in the distal dendrites; (d) The fine structure of the burst was typical of RE cells: the bursts were broad, they needed strong current pulses to be evoked, and the sodium spikes showed an *accelerando-decelerando* pattern (Fig. 16A); (e) Finally, the dendritic localization of  $I_T$  shaped the sensitivity of the cell to synaptic inputs and reproduced the typical patterns of responsiveness seen *in vivo* (see below).

The distribution of the membrane potential within an RE cell during the burst is apparent from the color coding in Fig. 16B. An LTS produced in the distal dendrites progressively "loads" the soma with current. The soma, in turn, produces sodium spikes that have a limited back-propagation to the dendrites. The consequence of the distal dendritic localization of  $I_T$  is the slowly-rising phase

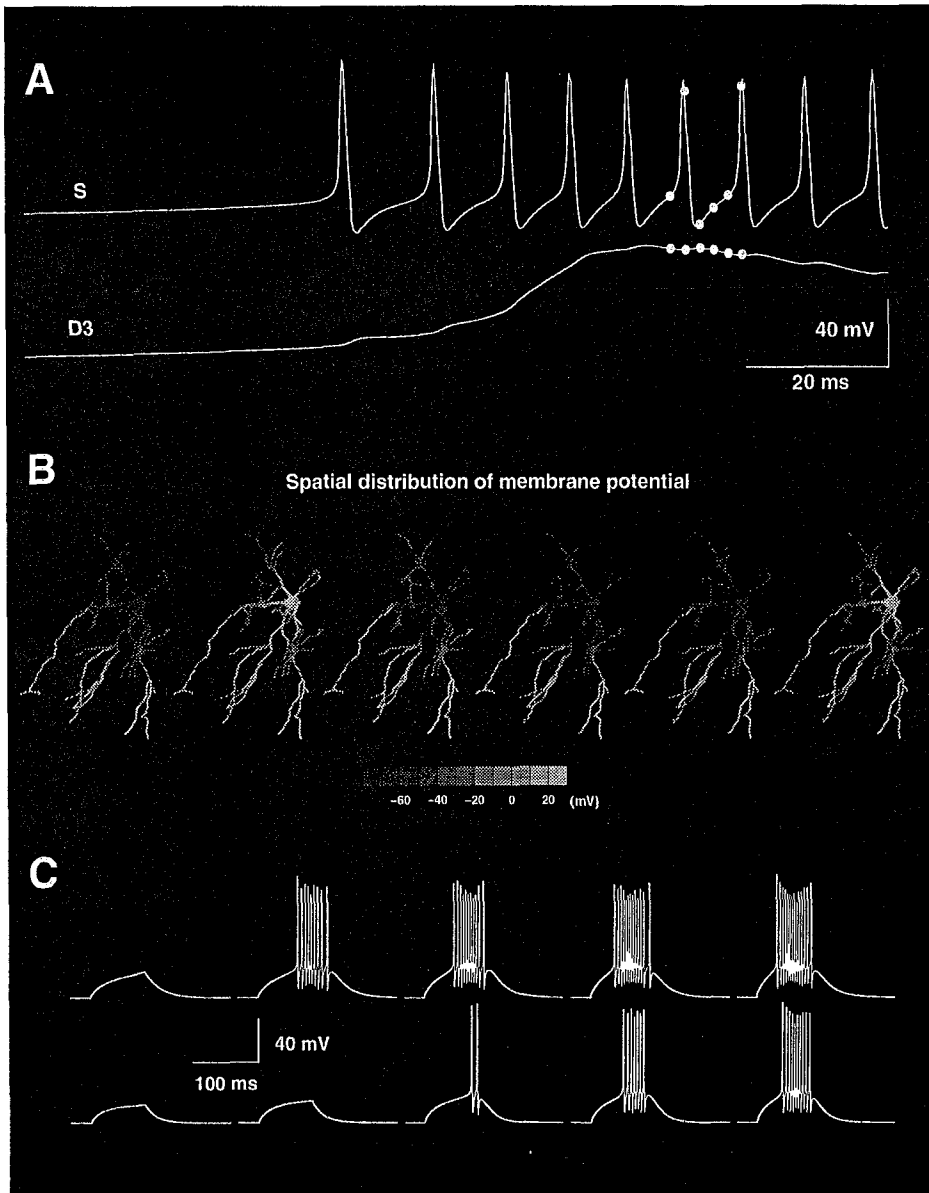


Figure 16:

Model of dendritically-generated bursts in thalamic reticular cells. A. Detail of the somatic and dendritic membrane potential during a burst. B. Distribution of the membrane potential during the burst as indicated by the color scale. The 6 successive frames correspond to the 6 circles indicated in A. C. Graded and all-or-none properties of RE bursts. The successive bursts from left to right were elicited by depolarizing pulses of increasing amplitudes, from  $-85 \text{ mV}$ . Top row: simulated all-or-none bursts in the intact RE cell with high density of  $I_T$  in distal dendrites. Bottom row: same simulation, showing the graded nature of the burst in the presence of a constant depolarizing current uniformly distributed in the dendrites (density of  $0.02 \text{ mS/cm}^2$  and  $-20 \text{ mV}$  reversal potential). In the latter case, the number of action potentials in the burst was proportional to the amplitude of the current pulse. Modified from Destexhe et al. (1996b).

of the burst and an *accelerando-decelerando* pattern of sodium spikes, as observed experimentally in RE cells (Domich et al., 1986; Contreras et al., 1993).

Perhaps the most important consequence of the dendritic localization of  $I_T$  is its influence on the response of the cell to synaptic inputs. In the absence of other currents, the cell produced an all-or-none burst response (Fig. 16C-top), typical of recordings in slices. In this case, the multicompartment model responded in a way that is qualitatively similar to that of a single-compartment RE cell. However, in the presence of a sustained depolarizing current in the dendrites, the bursts developed more gradually (Fig. 16C-bottom). For strong sustained currents, the cell may lose its ability to generate bursts. These properties are reminiscent of *in vivo* recordings from RE cells that show graded burst responses (Contreras et al., 1993). In this case, a single compartment model was unable to reproduce the results, even qualitatively.

These models and experiments suggest that dendritic T-current plays an important role in RE cells, especially *in vivo*. RE cells receive collaterals of almost all thalamo-cortical and cortico-thalamic fibers. It is possible that, by "sampling" the thalamocortical activity, RE cells adjust their tendency to produce bursts through an interplay of synaptic and  $I_T$  currents in the dendrites (Destexhe et al., 1996b).

## 9 SYNTHESIS

In this section, we synthesize the proposed mechanisms of thalamic rhythmicity that have been tested by modeling studies and show that they can be integrated into a uniform framework.

### SPINDLE RHYTHMICITY IN THE INTACT THALAMUS

In thalamic networks containing intact interactions between TC and RE cells, different models point to the conclusion that the intrinsic rebound burst properties of TC and RE cells, and the receptor types involved in the synaptic interactions between them, are a robust excitable system for generating oscillations (Fig. 17A). The membrane potentials of TC cells are typically around -60 to -70 mV and they receive strong IPSPs from RE cells. These IPSPs are ideally suited for triggering rebound bursts in TC cells (Deschênes et al., 1984; Steriade and Deschênes, 1984; Huguenard and Prince, 1994b; Warren et al., 1994; Bal et al., 1995a).

In RE cells, the resting levels of the membrane potential tend to be more hyperpolarized, and the EPSPs received from TC cells are powerful in generating bursts (Huguenard and Prince, 1992; Contreras et al., 1993; Huguenard and Prince, 1994b; Warren et al., 1994; Bal et al., 1995a). These properties create conditions that make the thalamus a highly efficient structure for in generating bursting oscillations. This scheme is also consistent with the mirror image between TC and RE bursts in the intact thalamus (Steriade and Llinás, 1988; von Krosigk et al., 1993; Bal et al., 1995a, 1995b).

The waxing-and-waning of spindle oscillations in the thalamus is consistent with the hypothesis that  $Ca^{2+}$  regulates the h-current in TC cells (Destexhe et al., 1993a, 1993b). This activity-dependent mechanism gradually limits the ability of the RE cell to evoke a rebound burst in the TC cell, which produces a state that is refractory to bursting. The postulated mechanism was based on voltage-clamp and current-clamp data in other preparations (Hagiwara and Irisawa, 1989; Schwindt et al., 1992). After a few consecutive bursts, the  $Ca^{2+}$ -induced augmentation of  $I_h$  conductance reduces the tendency of TC cells to produce rebound bursts, which progressively leads to the cessation of the oscillation. After a silent period of 10-20 s, the spontaneously oscillating TC cell starts

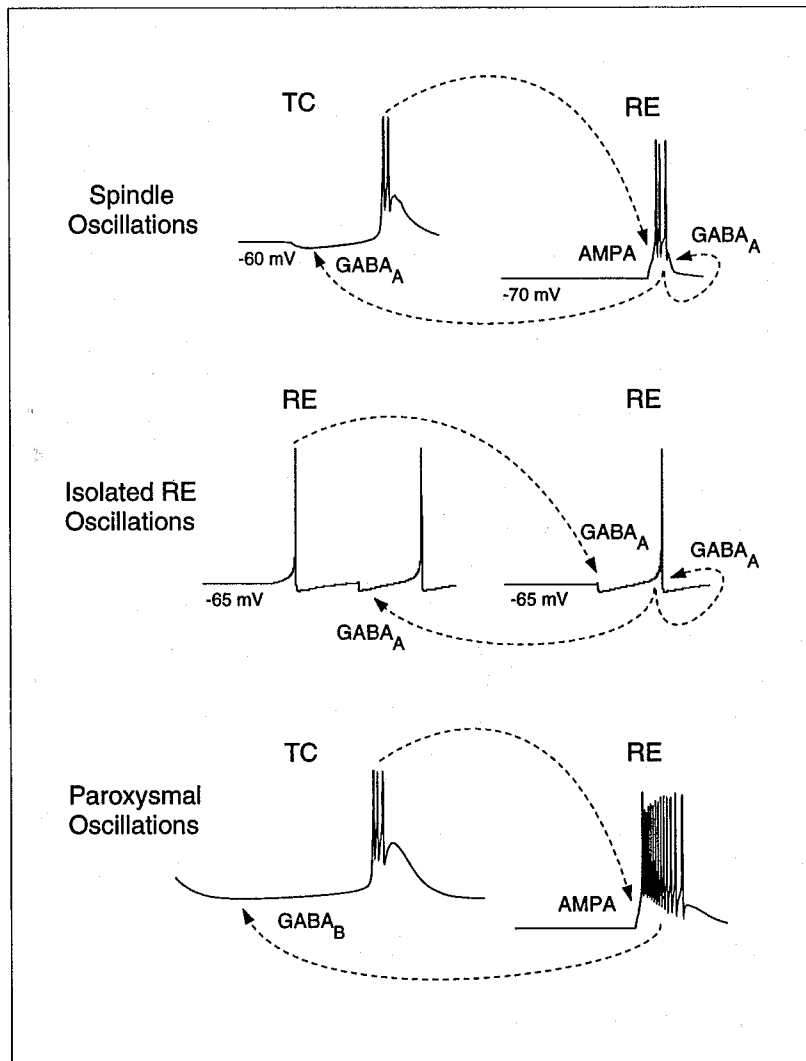


Figure 17:

Proposed mechanisms for different types of oscillations observed in the thalamic circuitry. *Top:* Spindle oscillations at  $\sim 10\text{ Hz}$  can result from the interaction between TC and RE cells. The TC cell is maintained at a depolarized level around  $-60\text{ mV}$  and the low-threshold spike can be elicited by  $\text{GABA}_A$ -dominated IPSPs arising from the RE cell. The RE cell has a more hyperpolarized membrane potential, such that LTSs can be triggered by  $\text{AMPA}$ -mediated EPSPs delivered from TC axons. *Middle:* Another type of oscillation at a similar frequency can occur between RE cells if they are maintained at a more depolarized level. In this case, LTSs can be produced in the RE cell following  $\text{GABA}_A$ -mediated IPSPs arising from neighboring RE cells. *Bottom:* Paroxysmal oscillations of  $\sim 3\text{ Hz}$  can be produced by TC-RE circuits if intra-RE  $\text{GABA}_A$ -mediated inhibition is suppressed. In this case the prolonged discharges of RE cells elicit  $\text{GABA}_B$ -dominated IPSPs in TC cells.

to oscillate and the cycle repeats. This is consistent with the augmentation of conductance in TC neurons at the end of a spindle sequence (Nuñez et al., 1992; Bal and McCormick, 1995), and the after-depolarization observed in the same cells following rebound bursts (Bal and McCormick, 1995).

*How are spindles initiated?* Spindle waves can be observed in the thalamus in the absence of cortical or prethalamic inputs, and in slices which lack all inputs. Several hypotheses have been proposed for the initiation of a spindle sequence. First, a region of the thalamus might be more excitable and spontaneous firing could start an oscillation (Kim et al., 1995). This is supported by a report that stimulation of a single RE cell could initiate a spindle wave in the whole network (Kim et al., 1995). Second, some spontaneously oscillating TC cells in an otherwise homogeneous network might recruit the whole network into spindle rhythmicity, as demonstrated in the model presented here. A single initiator TC cell was spontaneously active and recruited the rest of the network into spindle oscillations. As few as one initiator TC cell is needed in small networks of around a hundred thalamic cells. Blocking either excitatory or inhibitory transmission would result in a quiescent network, as observed experimentally (von Krosigk et al., 1993), except for the initiator cells, which should continue to display intrinsic oscillations. If several TC cells are needed to discharge one RE cell, then the network must wait for bursts to occur by chance in several TC cells simultaneously.

*How are spindles propagated?* A recent investigation of spindle waves in ferret thalamic slices (Kim et al., 1995) demonstrated that these oscillations propagate through the divergence of axonal connections between TC and RE cells. Models have been explored for how local recruitment could generate propagating waves of activity (Golomb et al., 1996; Destexhe et al. 1996a). At each cycle of the oscillation, the spindle propagates as more TC and RE cells are recruited. A steady propagation occurs if these projections are topographically organized between TC and RE cells, as appears to be the case from morphological studies (Minderhoud, 1971; Sanderson, 1971; Ohara and Lieberman, 1985; Fitzgibbon et al., 1995; Gonzalo-Ruiz and Lieberman, 1995).

Recent *in vivo* multielectrode recordings in cat association cortex indicate that spindles appear in near-simultaneity in cortical sites distant up to 7 mm (Contreras et al., 1995). A thalamo-cortical model indicates that the difference between propagating waves *in vitro* and simultaneity *in vivo* can be reconciled on the basis of the extended cortico-thalamic and thalamo-cortical projections (Destexhe et al., 1996c).

*How are spindles terminated?* There are several possible explanations. First, the observed refractoriness (Kim et al., 1995) of the thalamic network implies that there is a process that builds up and subsequently suppresses these oscillations. As proposed previously, an activity-dependent upregulation of  $I_h$  might fill this role (McCormick, 1992; Toth and Crunelli, 1992; Destexhe et al., 1993b; Bal and McCormick, 1995). Second, the termination might result from the progressive hyperpolarization of RE cells during a spindle sequence (von Krosigk et al., 1993). Third, there might be an activity-dependent depression of GABAergic currents (von Krosigk and McCormick, 1992; Kim et al., 1995). Fourth, *in vivo* data indicate that the waning of spindle waves is associated with a progressive desynchronization of the network (Contreras and Steriade, 1996), although this could also be a natural consequence of waning properties intrinsic to TC cells.

A model that explored the first of these possibilities was presented above. The proposed upregulation of  $I_h$  is consistent with a series of experimental results: (a) A few TC cells can display intrinsic waxing and waning oscillations (Leresche et al., 1991), and those are sensitive to  $I_h$  (Soltesz et al., 1991). These oscillations are characterized by an after depolarization (ADP) that lasts several seconds (Leresche et al., 1991). (b) A cesium-sensitive ADP was also observed in TC cells following a spindle sequence, consistent with an augmentation of  $I_h$  conductance (Bal and McCormick, 1995). (c) A progressive diminution of input resistance was measured in TC cells during the spindle

oscillation *in vivo* (Nunez et al., 1992). (d) Spindles triggered by electrical stimulation displayed a refractory period, as observed *in vitro* (Kim et al., 1995) and *in vivo* from cortically-elicited spindles (D. Contreras, A. Destexhe, T.J. Sejnowski and M. Steriade, unpublished results). (e) Colliding spindle waves do not cross but rather merge into a unique oscillation (Kim et al., 1995). (f) Spindle oscillations can be transformed into sustained oscillations following extracellular application of cesium (Bal and McCormick, 1995), most likely through a block of  $I_h$ . Taken together, these data are consistent with a progressive build-up of  $I_h$  during the spindle oscillation, until the TC cells can no longer be sufficiently hyperpolarized for the whole network to continue to oscillate. Whether this phenomenon is calcium-dependent or due to another second messenger system remains to be determined.

## OSCILLATIONS IN THE ISOLATED RETICULAR NUCLEUS

In our model of the RE nucleus, complete deafferentation produces natural state of quiescence with hyperpolarized resting potentials close to the reversal potential of GABA<sub>A</sub> IPSPs. Thus, RE cells interconnected through inhibitory synapses, acting on GABA<sub>A</sub> receptors, may not be able to sustain rebound bursts without the help of depolarization from other structures. This is consistent with the recordings in the deafferented RE nucleus in slices, for which spontaneous oscillations were not reported (Avanzini et al., 1989; Huguenard and Prince, 1992; von Krosigk et al., 1993; Huguenard and Prince, 1994b; Warren et al., 1994; Bal et al., 1995b).

However, the models further suggest that neuromodulation can make interconnected RE neurons oscillate in a sustained fashion (Fig. 17B). In the presence of a depolarizing neuromodulatory drive, such as that provided by noradrenaline, serotonin, or glutamate acting at metabotropic receptors, the resting level of RE cells is more depolarized (McCormick, 1992). In the model, when neuromodulation was included, that the same IPSPs that were ineffective in the absence of neuromodulation could trigger rebound bursts (Destexhe et al., 1994b). Interconnected RE cells therefore can oscillate via mutual inhibitory interactions if their resting level is sufficiently depolarized (Fig. 17B). This is consistent with observations of spindle rhythmicity in the isolated RE nucleus *in vivo* (Steriade et al., 1987).

In large networks of model RE cells with dense proximal connectivity, a collective oscillation can be sustained or suppressed, depending on the presence of neuromodulation. Waxing-and-waning was produced by the alternation of partially synchronized periods of oscillatory behavior with desynchronized periods (Destexhe et al., 1994a). This therefore suggests that spindle rhythmicity can exist in the isolated RE nucleus, but is based on different mechanisms than the spindles involving TC-RE interactions.

## PAROXYSMAL OSCILLATIONS

Models suggest that several factors are essential to account for paroxysmal burst patterns in the thalamic circuitry.

First, an oscillation at a frequency of 3-4 Hz arises from mutual recruitment of bursts in TC and RE cells (Fig. 17C). Rebound bursts are elicited following IPSPs in TC cells and EPSPs from TC cells evoke bursts in RE cells, similar to the mechanism for generating spindle oscillations. However, burst discharges are prolonged in both type of cells and strong GABA<sub>B</sub>-dominated IPSPs are seen in TC cells (Golomb et al., 1996; Destexhe et al. 1996a).

Second, prolonged burst patterns arise in both type of cells following the loss of lateral inhibition

in the RE nucleus. If this GABA<sub>A</sub>-mediated inhibition is suppressed, RE cells produce prolonged discharges, which in turn evoke strong GABA<sub>B</sub>-dominated IPSPs in TC cells (Fig 14). These strong IPSPs are then very efficient for rebound burst generation in TC cells due to a more pronounced deinactivation of the T-current.

Third, the enhanced GABA<sub>B</sub>-mediated responses in the model are due to the activation kinetics of the G-protein cascade underlying GABA<sub>B</sub> receptor-mediated responses. Strong stimuli are typically needed to activate detectable GABA<sub>B</sub>-mediated currents in thalamic (Huguenard and Prince, 1994b; Sánchez-Vives et al., 1995) and hippocampal slices (Dutar and Nicoll, 1988; Davies et al., 1990). These observations were reproduced in a model by requiring that several binding sites of G-proteins are needed to activate the  $K^+$  channels associated to GABA<sub>B</sub> receptors (Destexhe and Sejnowski, 1995).

Taken together, these experimental findings and simulations of models suggest a cellular mechanism that could account for the generation of paroxysmal discharges at around 3 Hz in the thalamus. Following removal of GABA<sub>A</sub>-mediated inhibition, the disinhibited RE cells generate prolonged burst discharges in response to EPSPs. These prolonged discharges evoke powerful GABA<sub>B</sub>-mediated IPSPs in TC cells, due to the particular properties of GABA<sub>B</sub> transduction mechanisms. Following these slow IPSPs, TC cells generate secure rebound bursts which re-excite RE cells and the cycle restarts. The resulting oscillation is around 3 Hz and exhibits a higher synchrony than that found in spindle waves.

## 10 CONCLUSION

Computational studies have been used to explore the mechanisms of thalamic rhythmicity starting with the seminal model introduced by Andersen and Rutjord (1964), who predicted the significance of inhibitory rebound bursts. Several models of spindle rhythmicity have been proposed recently for the isolated reticular nucleus (Destexhe et al., 1994a; Golomb et al., 1994) as well as for the bidirectional interaction between TC and RE cells (Destexhe et al., 1993b, 1996a; Golomb et al., 1996). Without firm ties to experimental measurements, however, these models are difficult to verify. By using computational models based on physiological and biophysical data, it has been possible to generate plausible hypotheses and decisive predictions to test them. We have shown here how experimental data from different preparations, sometimes with apparently contrasting results, can be reconciled and used to illuminate different facets of the same framework.

## Acknowledgments

We acknowledge Drs. T. Bal, D. Contreras, J. Huguenard, D.A. McCormick and M. Steriade for kindly making their data available to us. We also thank them, as well as Drs. A. Babloyantz, D. Golomb, W.W. Lytton, J. Rinzel and X.J. Wang for many stimulating discussions. This research was supported by the Medical Research Council of Canada, Fonds de la Recherche en Santé du Québec, the Howard Hughes Medical Institute and the Office for Naval Research.

## References

- Akasu, T. and Tokimasa, T. (1992) Cellular metabolism regulating H and M currents in bullfrog sympathetic ganglia. *Canadian J. Physiol. Pharmacol.* **70** Suppl: S51-S55.
- Andersen, P. and Andersson, S.A. (1968) *Physiological Basis of the Alpha Rhythm*. Appelton Century Crofts, New York.
- Andersen, P. and Rutjord, T. (1964) Simulation of a neuronal network operating rhythmically through recurrent inhibition. *Nature (Lond.)* **204**: 289-190.
- Avanzini, G., M. de Curtis, F. Panzica and R. Spreafico. (1989) Intrinsic properties of nucleus reticularis thalami neurones of the rat studied in vitro. *J. Physiol. Lond.* **416**: 111-22.
- Avoli, M., Gloor, P., Kostopoulos, G. and Naquet, R. (1990) *Generalized Epilepsy*. Birkhäuser, Boston.
- Bal, T. and D.A. McCormick. (1993) Mechanisms of oscillatory activity in guinea-pig nucleus reticularis thalami *in vitro*: a mammalian pacemaker. *J. Physiol. (London)*, **468**: 669-691.
- Bal, T. and McCormick, D.A. (1995) A mechanism for the waning of thalamic spindle and "absence seizure-like" oscillations *in vitro*. *Soc. Neurosci. Abstracts* **21**: 11.
- Bal, T., von Krosigk, M. and McCormick, D.A. (1995a) Synaptic and membrane mechanisms underlying synchronized oscillations in the ferret LGNd *in vitro*. *J. Physiol. (London)* **483**: 641-663.
- Bal, T., von Krosigk, M. and McCormick, D.A. (1995b) Role of the ferret perigeniculate nucleus in the generation of synchronized oscillations *in vitro*. *J. Physiol. (London)* **483**: 665-685.
- Boland, L.M. and Bean, B.P. (1993) Modulation of N-type calcium channels in bullfrog sympathetic neurons by luteinizing hormone-releasing hormone: kinetics and voltage dependence. *J. Neurosci.* **13**: 516-533.
- Colquhoun, D., Jonas, P., and Sakmann, B. (1992) Action of brief pulses of glutamate on AMPA/KAINATE receptors in patches from different neurons of rat hippocampal slices. *J. Physiol. (London)* **458**, 261-287.
- Contreras, D., Curró Dossi, R. and Steriade, M. (1993) Electrophysiological properties of cat reticular thalamic neurones *in vivo*. *J. Physiol. (London)* **470**: 273-294.
- Contreras, D., Destexhe, A., Sejnowski, T.J. and Steriade, M. (1995) Synchronization of thalamic spindle oscillations is enhanced by cortical feedback input. *Soc. Neurosci. Abstracts* **21**: 1187.
- Contreras, D. and Steriade, M. (1996) Spindle oscillation in cats: the role of corticothalamic feedback in a thalamically-generated rhythm. *J. Physiol. (London)* **490**: 159-179.
- Coulter, D.A., Huguenard, J.R. and Prince, D.A. Calcium currents in rat thalamocortical relay neurones: kinetic properties of the transient, low-threshold current. (1989) *J. Physiol. (London)* **414**: 587-604.

- Crunelli, V., Soltesz, I., Toth, T.I., Turner, J. and Leresche, N. (1993) Intrinsic low-frequency oscillations of thalamocortical cells and their modulation by synaptic potentials. In: *Thalamic Networks for Relay and Modulation*; Miniciacchi, A., Molinari, M., Macchi, G. and Jones, E.G. (Ed.), pp. 375-384, Pergamon press, New York.
- Cucchiaro, J.B., Uhrich, D.J. and Sherman, S.M. (1991) Electron-microscopic analysis of synaptic input from the perigeniculate nucleus to the A-laminae of the lateral geniculate nucleus in cats. *J. Comp. Neurol.* **310**: 316-336.
- Curró Dossi, R., Nuñez, A. and Steriade, M. (1992) Electrophysiology of a slow (0.5-4 Hz) intrinsic oscillation of cat thalamocortical neurones *in vivo*. *J. Physiol. (London)* **447**: 215-234.
- Davies C.H., Davies, S.N. and Collingridge, G.L. (1990) Paired-pulse depression of monosynaptic GABA-mediated inhibitory postsynaptic responses in rat hippocampus. *J. Physiol.* **424**: 513-531.
- Deschênes, M., Paradis, M., Roy, J.P. and Steriade, M. (1984) Electrophysiology of neurons of lateral thalamic nuclei in cat: resting properties and burst discharges. *J. Neurophysiol.* **55**: 1196-1219.
- Destexhe, A. and Babloyantz, A. (1992) Cortical coherent activity induced by thalamic oscillations. In: *Neural Network Dynamics*; Taylor, J.G., Caianello, E.R., Cotterill, R.M.J., and Clark, J.W. (Ed.), pp. 234-249, Springer-Verlag, Berlin.
- Destexhe, A. and Babloyantz, A. (1993) A model of the inward current  $I_h$  and its possible role in thalamocortical oscillations. *NeuroReport* **4**: 223-226.
- Destexhe, A. and Sejnowski, T.J. (1995) G-protein activation kinetics and spill-over of GABA may account for differences between inhibitory responses in the hippocampus and thalamus. *Proc. Natl. Acad. Sci. USA* **92**: 9515-9519.
- Destexhe, A., Babloyantz, A. and Sejnowski, T.J. (1993a) Ionic mechanisms for intrinsic slow oscillations in thalamic relay neurons. *Biophys. J.* **65**: 1538-1552.
- Destexhe, A., McCormick, D.A. and Sejnowski, T.J. (1993b) A model for 8-10 Hz spindling in interconnected thalamic relay and reticularis neurons. *Biophys. J.* **65**: 2474-2478.
- Destexhe, A., Contreras, D., Sejnowski, T.J. and Steriade, M. (1994a) A model of spindle rhythmicity in the isolated thalamic reticular nucleus. *J. Neurophysiol.* **72**: 803-818.
- Destexhe, A., Contreras, D., Sejnowski, T.J. and Steriade, M. (1994b) Modeling the control of reticular thalamic oscillations by neuromodulators. *NeuroReport* **5**: 2217-2220.
- Destexhe, A., Mainen, Z. and Sejnowski, T.J. (1994c) An Efficient Method for Computing Synaptic Conductances Based on a Kinetic Model of Receptor Binding. *Neural Computation* **6**: 14-18.
- Destexhe, A., Mainen, Z. and Sejnowski, T.J. (1994d) Synthesis of models for excitable membranes, synaptic transmission and neuromodulation using a common kinetic formalism. *J. Computational Neurosci.* **1**: 195-231.

- Destexhe, A., Bal, T., McCormick, D.A., and Sejnowski, T.J. (1996a) Ionic mechanisms underlying synchronized oscillations and propagating waves in a model of ferret thalamic slices. *J. Neurophysiol.*, in press.
- Destexhe, A., Contreras, D., Steriade, M., Sejnowski, T.J., and Huguenard, J.R. (1996b) In vivo, in vitro and computational analysis of dendritic calcium currents in thalamic reticular neurons. *J. Neurosci.* **16**: 169-185.
- Destexhe, A., Contreras, D., Sejnowski, T.J. and Steriade, M. (1996c) Cortical projections to the thalamic reticular nucleus may control the spatiotemporal coherence of spindle and epileptic oscillations. *Society for Neuroscience Abstracts* **22**, in press.
- DiFrancesco, D. and Mangoni, M. (1994) Modulation of single hyperpolarization-activated channels (i(f)) by cAMP in the rabbit sino-atrial node. *J. Physiol.* **474**: 473-482.
- Domich, L., Oakson, G. and Steriade, M. (1986) Thalamic burst patterns in the naturally sleeping cat: a comparison between cortically projecting and reticularis neurones. *J. Physiol.* **379**: 429-449.
- Dutar, P. and Nicoll, R.A. (1988) A physiological role for GABAB receptors in the central nervous system. *Nature* **332**: 156-158.
- Fitzgibbon, T., Tevah, L.V. and Jervie-Sefton, A. (1995) Connections between the reticular nucleus of the thalamus and pulvinar-lateralis posterior complex: a WGA-HRP study. *J. Comp. Neurol.* **363**: 489-504.
- Gloor, P., Avoli, M. and Kostopoulos, G. (1990) Thalamocortical relationships in generalized epilepsy with bilateral synchronous spike-and-wave discharge. In: *Generalized Epilepsy*, Avoli, M., Gloor, P., Kostopoulos, G. and Naquet, R. (Ed), pp. 190-212, Birkhäuser, Boston.
- Golard, A. and Siegelbaum, S.A. (1993) Kinetic basis for the voltage-dependent inhibition of N-type calcium current by somatostatin and norepinephrine in chick sympathetic neurons. *J. Neurosci.* **13**: 3884-3894.
- Golomb, D. and Rinzel, J. (1994) Clustering in globally coupled inhibitory neurons. *Physica D* **72**: 259-282.
- Golomb, D., Wang, X.J. and Rinzel, J. (1994) Synchronization properties of spindle oscillations in a thalamic reticular nucleus model. *J. Neurophysiol.* **72**: 1109-1126.
- Golomb, D., Wang, X.J. and Rinzel, J. (1996) Propagation of spindle waves in a thalamic slice model. *J. Neurophysiol.* **75**: 750-769.
- Gonzalo-Ruiz, A. and Lieberman, A.R. (1995) Topographic organization of projections from the thalamic reticular nucleus to the anterior thalamic nuclei in the rat. *Brain Res. Bull.* **37**: 17-35.
- Hagiwara, N. and Irisawa, H. (1989) Modulation by intracellular  $Ca^{2+}$  of the hyperpolarization-activated inward current in rabbit single sino-atrial node cells. *J. Physiol. (London)* **409**: 121-141.

- Harris, R.M. (1987) Axon collaterals in the thalamic reticular nucleus from thalamocortical neurons of the rat ventrobasal thalamus. *J. Comp. Neurol.* **258**: 397-406.
- Hille B (1992) *Ionic Channels of Excitable Membranes*. Sinauer Associates INC, Sunderland, MA.
- Hindmarsh, J.L. and Rose, R.M. (1994a) A model for rebound bursting in mammalian neurons. *Phil. Trans. Roy. Soc. Lond. B* **346**: 129-150.
- Hindmarsh, J.L. and Rose, R.M. (1994b) A model of intrinsic and driven spindling in thalamocortical neurons. *Phil. Trans. Roy. Soc. Lond. B* **346**: 165-183.
- Hosford, D.A., Clark, S., Cao, Z., Wilson, W.A. Jr., Lin, F.H., Morrisett, R.A. and Huin, A. (1992) The role of GABA<sub>B</sub> receptor activation in absence seizures of lethargic (lh/lh) mice. *Science (Wash.)* **257**: 398-401.
- Huguenard, J.R. and McCormick, D.A. (1992) Simulation of the currents involved in rhythmic oscillations in thalamic relay neurons. *J. Neurophysiol.* **68**: 1373-1383.
- Huguenard, J.R. and Prince, D.A. (1992) A novel T-type current underlies prolonged calcium-dependent burst firing in GABAergic neurons of rat thalamic reticular nucleus. *J. Neurosci.* **12**: 3804-3817.
- Huguenard, J.R. and Prince, D.A. (1994a) Clonazepam suppresses GABA(B)-mediated inhibition in thalamic relay neurons through effects in nucleus reticularis. *J. Neurophysiol.* **71**: 2576-2581.
- Huguenard, J.R. and Prince, D.A. (1994b) Intrathalamic rhythmicity studied *in vitro*: nominal T-current modulation causes robust anti-oscillatory effects. *J. Neurosci.* **14**: 5485-5502.
- Hodgkin, A.L. and Huxley, A.F. (1952) A quantitative description of membrane current and its application to conduction and excitation in nerve. *J. Physiol. (London)* **117**: 500-544.
- Ingram, S.L. and Williams, J.T. (1994) Opioid inhibition of Ih via adenylyl cyclase. *Neuron* **13**: 179-186.
- Jahnsen, H. and Llinás, R.R. (1984a) Electrophysiological properties of guinea-pig thalamic neurons: an *in vitro* study. *J. Physiol.* **349**: 205-226.
- Jahnsen, H. and Llinás, R.R. (1984b) Ionic basis for the electroresponsiveness and oscillatory properties of guinea-pig thalamic neurons *in vitro*. *J. Physiol.* **349**: 227-247.
- Jones, E.G. (1985) *The Thalamus*. Plenum Press, New York.
- Kim, U., Bal, T. and McCormick, D.A. (1995) Spindle waves are propagating synchronized oscillations in the ferret LGNd *in vitro*. *J. Neurophysiol.* **74**: 1301-1323.
- Kopell, N. and LeMasson, G. (1994) Rhythmogenesis, amplitude modulation, and multiplexing in a cortical architecture. *Proc. Natl. Acad. Sci. USA* **91**: 10586-10590.
- Legendre, P., Rosenmund, C. and Westbrook, G.L. (1993) Inactivation of NMDA channels in cultured hippocampal neurons by intracellular calcium. *J. Neurosci.* **13**: 674-684.

- Leresche, N., Jassik-Gerschenfeld, D., Haby M., Soltesz, I. and Crunelli, V. (1990) Pacemaker-like and other types of spontaneous membrane potential oscillations in thalamocortical cells. *Neurosci. Lett.* **113**: 72-77.
- Leresche, N., Lightowler, S., Soltesz, I., Jassik-Gerschenfeld, D. and Crunelli, V. (1991) Low frequency oscillatory activities intrinsic to rat and cat thalamocortical cells. *J. Physiol.* **441**: 155-174.
- Liu, Z., Vergnes, M., Depaulis, A. and Marescaux, C. (1992) Involvement of intrathalamic GABA<sub>B</sub> neurotransmission in the control of absence seizures in the rat. *Neuroscience* **48**: 87-93.
- Liu, X.B., Warren, R.A. and Jones, E.G. (1995) Synaptic distribution of afferents from reticular nucleus in ventroposterior nucleus of cat thalamus. *J. Comp. Neurol.* **352**: 187-202.
- Lytton, W.W. and Sejnowski, T.J. (1992) Computer model of ethosuximide's effect on a thalamic cell. *Annals Neurol.* **32**: 131-139.
- Lytton, W.W., Contreras, D., Destexhe, A. and Steriade, M. (1996a) Nucleus reticularis thalami controls the quiescence of thalamocortical neurons during seizures in a computer network model. *Society for Neuroscience Abstracts* **22**, in press.
- Lytton, W.W., Destexhe, A. and Sejnowski, T.J. (1996b) Control of slow oscillations in the thalamocortical neuron: a computer model. *Neuroscience* **70**: 673-684.
- MacNeil, S., Lakey, T. and Tomlinson, S. (1985) Calmodulin regulation of adenylate cyclase activity. *Cell Calcium* **6**: 213-216.
- McCormick, D.A. (1992) Neurotransmitter actions in the thalamus and cerebral cortex and their role in neuromodulation of thalamocortical activity. *Prog. Neurobiol.* **39**: 337-388.
- McCormick, D.A. and Huguenard, J.R. (1992) A model of the electrophysiological properties of thalamocortical relay neurons. *J. Neurophysiol.* **68**: 1384-1400.
- McCormick, D.A. and Pape, H.C. (1990a) Properties of a hyperpolarization-activated cation current and its role in rhythmic oscillations in thalamic relay neurones. *J. Physiol.* **431**: 291-318.
- McCormick, D.A. and Pape, H.C. (1990b) Noradrenergic modulation of a hyperpolarization-activated cation current in thalamic relay neurones. *J. Physiol.* **431**: 319-342.
- McCormick, D.A. and Prince, D.A. (1986) Acetylcholine induces burst firing in thalamic reticular neurones by activating a potassium conductance. *Nature (London)* **319**: 402-405.
- McCormick, D.A. and Wang, Z. (1991) Serotonin and noradrenaline excite GABAergic neurones of the guinea-pig and cat nucleus reticularis thalami. *J. Physiol.* **442**: 235-255.
- McCormick, D.A. and Williamson, A. (1991) Modulation of neuronal firing mode in cat and guinea pig LGNd by histamine: possible cellular mechanisms of histaminergic control of arousal. *J. Neurosci.* **11**: 3188-3199.
- Minderhoud, J.M. (1971) An anatomical study of the efferent connections of the thalamic reticular nucleus. *Exp. Brain Res.* **112**: 435-446.

- Morison, R.S. and Basset, D.L. (1945) Electrical activity of the thalamus and basal ganglia in decorticate cats. *J. Neurophysiol.* **8**: 309-314.
- Muhlethaler, M. and Serafin, M. Thalamic spindles in an isolated and perfused preparation in vitro. *Brain Res.* **524**: 17-21, 1990.
- Nuñez, A., Curro-Dossi, R., Contreras, D. and Steriade, M. (1992) Intracellular evidence for incompatibility between spindle and delta oscillations in thalamocortical neurons of cat. *Neuroscience* **48**: 75-85.
- Ohara, P.T. and Lieberman, A.R. (1985) The thalamic reticular nucleus of the adult rat: experimental anatomical studies. *J. Neurocytol.* **14**: 365-411.
- Pape, H.C. (1992) Adenosine promote burst activity in guinea-pig geniculocortical neurones through two different ionic mechanisms. *J. Physiol. Lond.* **447**: 729-753.
- Perkel, D.H. and Mulloney, B. (1974) Motor pattern production in reciprocally inhibitory neurons exhibiting postinhibitory rebound. *Science* **185**: 181-183.
- Pinault, D., Bourassa, J. and Deschênes, M. (1995) The axonal arborization of single thalamic reticular neurons in the somatosensory thalamus of the rat. *Eur. J. Neurosci.* **7**: 31-40.
- Pollard, C.E. and Crunelli, V. (1988) Intrinsic membrane currents in projection cells of the cat and rat lateral geniculate nucleus. *Neurosci. Lett.* **32**: S39.
- Rose, R.M. and Hindmarsh, J.L. (1985) A model of a thalamic neuron. *Proc. R. Soc. Lond. B* **225**: 161-193.
- Rose, R.M. and Hindmarsh, J.L. (1989) The assembly of ionic currents in a thalamic neuron. I. The three-dimensional model. *Proc. R. Soc. Lond. B Biol. Sci.* **237**: 267-288.
- Rowat, P.F. and Selverston, A.I. (1993) Modeling the gastric mill central pattern generator of the lobster with a relaxation-oscillator network. *J. Neurophysiol.* **70**: 1030-1053.
- Sánchez-Vives, M.V., Bal, T. and McCormick, D.A. (1995) Properties of GABAergic inhibition in the ferret LGNd contributing to the generation of synchronized oscillations. *Soc. Neurosci. Abstracts* **21**: 11.
- Sanderson, K.J. (1971) The projection of the visual field to the lateral geniculate and medial interlaminar nuclei in the cat. *J. Comp. Neurol.* **143**: 101-108.
- Schwindt, P.C., Spain, W.J. and Crill, W.E. (1992) Effects of intracellular calcium chelation on voltage-dependent and calcium-dependent currents in cat neocortical neurons. *Neuroscience* **47**: 571-578.
- Selverston, A.I. (1985) *Model Neural Networks and Behavior*. New York: Plenum Press, 1985.
- Solomon, J.S. and Nerbonne, J.M. (1993) Two kinetically distinct components of hyperpolarization-activated current in rat superior colliculus-projecting neurons. *J. Physiol.* **469**: 291-313.

- Solomon, J.S., Doyle, J.F., Burkhalter, A. and Nerbonne, J.M. (1993) Differential expression of hyperpolarization-activated currents reveals distinct classes of visual cortical projection neurons. *J. Neurosci.* **13**: 5082-5091.
- Soltesz, I. and Crunelli, V. (1992) GABA<sub>A</sub> and pre- and post-synaptic GABA<sub>B</sub> receptor-mediated responses in the lateral geniculate nucleus. *Progr. Brain Res.* **90**: 151-169.
- Soltesz, I., Lightowler, S., Leresche, N., Jassik-Gerschenfeld, D., Pollard, C.E. and Crunelli, V. (1991) Two inward currents and the transformation of low frequency oscillations of rat and cat thalamocortical cells. *J. Physiol. Lond.* **441**: 175-197.
- Steriade, M. and Deschênes, M. (1984) The thalamus as a neuronal oscillator. *Brain Res. Rev.* **8**: 1-63.
- Steriade, M. and Llinás, R.R. (1988) The functional states of the thalamus and the associated neuronal interplay. *Physiol. Reviews* **68**: 649-742.
- Steriade, M., Deschênes, M., Domich, L. and Mulle, C. (1985) Abolition of spindle oscillations in thalamic neurons disconnected from nucleus reticularis thalami. *J. Neurophysiol.* **54**: 1473-1497.
- Steriade, M., Domich, L., Oakson, G. and Deschênes, M. (1987) The deafferented reticular thalamic nucleus generates spindle rhythmicity. *J. Neurophysiol.* **57**: 260-273.
- Steriade, M., Jones, E.G. and Llinás, R.R. (1990) *Thalamic Oscillations and Signalling*. John Wiley and Sons, New York.
- Steriade M., McCormick D.A. and Sejnowski T.J. (1993a) Thalamocortical oscillations in the sleeping and aroused brain. *Science (Wash.)* **262**: 679-685.
- Steriade, M., Contreras, D., Curró Dossi, R. and Nuñez, A. (1993b) The slow (< 1 Hz) oscillation in reticular thalamic and thalamocortical neurons: scenario of sleep rhythm generation in interacting thalamic and neocortical networks. *J. Neurosci.* **13**: 3284-3299.
- Toth, T. and Crunelli, V. (1992) Computer simulations of the pacemaker oscillations of thalamocortical cells. *NeuroReport* **3**: 65-68.
- Uhlich, D.J., Cucchiaro, J.B., Humphrey, A.L. and Sherman S.M. (1991) Morphology and axonal projection patterns of individual neurons in the cat perigeniculate nucleus. *J. Neurophysiol.* **65**: 1528-1541.
- VanDongen, A.M.J., Codina, J., Olate, J., Mattera, R., Joho, R., Birnbaumer, L. and Brown, A.M. (1988) Newly identified brain potassium channels gated by the guanine nucleotide binding protein G<sub>o</sub>. *Science* **242**: 1433-1437.
- Verzeano, M. and Negishi, K. (1960) Neuronal activity in cortical and thalamic networks. A study with multiple microelectrodes. *J. Gen. Physiol.* **43**: 177-195.
- Verzeano, M., Laufer, M., Spear, P. and McDonald, S. (1965) L'activité des réseaux neuroniques dans le thalamus du singe. *Actualités Neurophysiologiques* **6**: 223-251.
- von Krosigk, M., Bal, T. and McCormick, D.A. (1993) Cellular mechanisms of a synchronized oscillation in the thalamus. *Science* **261**: 361-364.

- Wallenstein, G.V. (1994a) A model of the electrophysiological properties of nucleus reticularis thalami neurons. *Biophys. J.* **66**: 978-988.
- Wallenstein, G.V. (1994b) The role of thalamic IGABAB in generating spike-wave discharges during petit mal seizures. *Neuroreport* **5**: 1409-1412.
- Wallenstein, G.V. (1995) Adenosinic modulation of 7-14 Hz spindle rhythms in interconnected thalamic relay and nucleus reticularis neurons. Submitted.
- Wang, X.J. (1994) Multiple dynamical modes of thalamic relay neurons: rhythmic bursting and intermittent phase-locking. *Neuroscience* **59**: 21-31.
- Wang, X.J. and Rinzel, J. (1992) Alternating and synchronous rhythms in reciprocally inhibitory model neurons. *Neural Computation* **4**: 84-97.
- Wang, X.J. and Rinzel, J. (1993) Spindle rhythmicity in the reticularis thalami nucleus – synchronization among inhibitory neurons. *Neuroscience* **53**: 899-904.
- Wang, X.J., Rinzel, J. and Rogawski, M.A. (1991) A model of the T-type calcium current and the low-threshold spike in thalamic neurons. *J. Neurophysiol.* **66**: 839-850.
- Wang, X.J., Golomb, D. and Rinzel, J. (1995) Emergent spindle oscillations and intermittent burst firing in a thalamic model: specific neuronal mechanisms. *Proc. Natl. Acad. Sci. USA* **92**: 5577-5581.
- Warren, R.A., Agmon, A. and Jones, E.G. (1994) Oscillatory synaptic interactions between ventro-posterior and reticular neurons in mouse thalamus *in vitro*. *J. Neurophysiol.* **72**: 1993-2003.
- Yamada, M., Jahangir, A., Hosoya, Y., Inanobe, A., Katada, T. and Kurachi, Y. (1993) GK\* and brain G beta gamma activate muscarinic K<sup>+</sup> channel through the same mechanism. *J. Biol. Chem.* **268**: 24551-24554.
- Zaza, A., Maccaferri, G., Mangoni, M. and DiFrancesco, D. Intracellular calcium does not directly modulate cardiac pacemaker (if) channels. *Pflug. Archiv. Eur. J. Physiol.* **419**: 662-664, 1991.